



Review

CO₂ Derivatives of Molecular Tin Compounds. Part 1: Hemicarbonato and Carbonato Complexes †

Laurent Plasseraud

Institut de Chimie Moléculaire de l'Université de Bourgogne (ICMUB), UMR-CNRS 6302,
Université de Bourgogne Franche-Comté, 9 avenue A. Savary, F-21078 Dijon, France;
laurent.plasseraud@u-bourgogne.fr

† Paper dedicated to Professor Georg Süss-Fink on the occasion of his 70th birthday.

Received: 31 March 2020; Accepted: 24 April 2020; Published: 29 April 2020



Abstract: This review focuses on organotin compounds bearing hemicarbonato and carbonato ligands, and whose molecular structures have been previously resolved by single-crystal X-ray diffraction analysis. Most of them were isolated within the framework of studies devoted to the reactivity of tin precursors with carbon dioxide at atmospheric or elevated pressure. Alternatively, and essentially for the preparation of some carbonato derivatives, inorganic carbonate salts such as K₂CO₃, Cs₂CO₃, Na₂CO₃ and NaHCO₃ were also used as coreagents. In terms of the number of X-ray structures, carbonate compounds are the most widely represented (to date, there are 23 depositions in the Cambridge Structural Database), while hemicarbonato derivatives are rarer; only three have so far been characterized in the solid-state, and exclusively for diorganotin complexes. For each compound, the synthesis conditions are first specified. Structural aspects involving, in particular, the modes of coordination of the hemicarbonato and carbonato moieties and the coordination geometry around tin are then described and illustrated (for most cases) by showing molecular representations. Moreover, when they were available in the original reports, some characteristic spectroscopic data are also given for comparison (in table form). Carbonato complexes are arbitrarily listed according to their decreasing number of hydrocarbon substituents linked to tin atoms, namely tri-, di-, and mono-organotins. Four additional examples, involving three CO₂ derivatives of C,N-chelated stannoxanes and one of a trinuclear nickel cluster Sn-capped, are also included in the last part of the chapter.

Keywords: tin complexes; carbon dioxide fixation; hypervalent compounds; X-ray crystallography

1. Introduction

Over the past fifty years, the coordination of CO₂ on metal centers has aroused great interest, mobilizing numerous groups around the world; even today, it continues to fascinate the community of inorganic and organometallic chemists. Pioneering works in this area are to be credited to M. E. Vol'pin et al., who highlighted in 1969 the formation of a rhodium-phosphine complex with a carbon dioxide adduct [1]. To our knowledge, the first resolution of an X-ray crystal structure showing the metal-coordination of a CO₂ molecule is to be attributed to M. Aresta et al., for the characterization of a nickel complex stabilized by triscyclohexylphosphines [2]. Since then, a multitude of CO₂ coordination modes has been revealed at the solid state, showing an important diversity of structures and involving most of transition metal atoms [3,4]. Knowledge in the field has regularly been reviewed and updated [5]. Nature has also been an important source of inspiration for chemists in this area. Thus, the zinc-based active site of carbonic anhydrase has been widely used as a model for the design of metal complexes in order to mimic the catalytic role of the enzyme toward carbon dioxide [6].

Nowadays, the organometallic chemistry of metal–CO₂ complexes remains a topical research area which is closely linked to the fields of materials (CO₂-capture) and catalysis (CO₂-transformation). Indeed, beyond the purely fundamental aspect, CO₂-coordination on a metallic center can be viewed as a key-step facilitating its activation and conversion into useful chemicals. In this way, carbon dioxide appears to be a potential renewable C1 raw material, rather than a waste, offering new opportunities for chemical reactions [7–9]. Currently, a great level of attention is being paid to the design of porous coordination polymers (PCPs) or metal–organic frameworks (MOF), owing to their absorption properties [10], but also transforming CO₂ [11]. Thus, the chemical utilization of carbon dioxide has become a crucial issue, in particular in view of the environmental challenges that humanity has to face, i.e., (i) the depletion of fossil carbon resources, and (ii) the continuous increase in CO₂ emissions and its consequences on the climate.

From a coordination chemistry point of view, the reactivity of main group metal elements (groups 13–15) with carbon dioxide has been, up to now, relatively underreviewed in the literature. Within the framework of our previous studies in this field, and using the support of the online portal of the Cambridge Structural Database (WebCSD) [12], we herein focus specifically on an inventory of X-ray crystallographic structures of tin compounds resulting from reactivity with carbon dioxide. To the best of our knowledge, tin complexes directly bearing a CO₂-coordinated molecule have never been isolated in the solid state. However, CO₂-adducts of tin complexes exist in the form of hemicarbonato, carbonato, carbamato, formate and phosphinoformate derivatives, and are generally obtained from insertion reactions by reacting carbon dioxide (under atmospheric pressure or requiring high pressure) with precursors having Sn–X bonds (X = O, N, H, P). In some cases, alternatively, inorganic carbonate salts are also used as reagents. Herein, we will focus exclusively on hemicarbonato and carbonato tin derivatives. These two distinct families of compounds are successively detailed thereafter, with a particular focus upon the synthetic and structural aspects. This inventory highlights the hypervalence of tin atoms in hemicarbonato and carbonato derivatives, which preferentially adopt penta- and hexa-coordination modes, with trigonal bipyramidal and octahedral geometries, respectively. An example of a heptacoordinated tin atom is also described in Section 3.2, which is devoted to carbonato tin complexes. In addition, and when they were available in the original publications, the relevant spectroscopic data resulting from the CO₂ reactivity (in particular, IR, ¹¹⁹Sn and ¹³C NMR in solution and in solid state) are also specified. For comparison, summary tables of structural and spectroscopic data are presented at the end of each section (Tables 1–10). The other aforementioned CO₂-adduct families, i.e., carbamato-, formato- and phosphino- formato complexes, are not included herein and will be the subject of a later inventory.

2. Hemicarbonato Tin Complexes

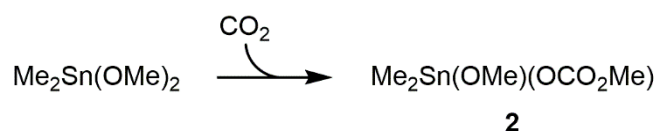
The synthesis of linear organic carbonates, also called carbonic esters, (RO)₂CO, from carbon dioxide and alcohols attracted a lot of attention during the 1990s and 2000s. This reaction, which is based on the direct use of CO₂ as a C1-synthon (Scheme 1), also has the advantage of producing only water as a byproduct. Thus, this synthesis pathway, leading to organic carbonates, fits well with the concept of sustainable chemistry and constitutes a safer and greener alternative route compared to historical uses involving phosgene and carbon monoxide [13].



Scheme 1. Reaction scheme leading to dialkyl carbonates from carbon dioxide and alcohols.

Most previous academic studies on the topic focused on the direct synthesis of dimethyl carbonate (DMC with R = –CH₃), the simplest of the linear organic carbonates, by reacting directly CO₂ with methanol. Indeed, in addition to being a model reaction, DMC is considered a green and environmentally sustainable molecule [14], usable as a solvent as well as a reagent in numerous applications, e.g., for biodiesel production [15]. Thus, numerous investigations involving the use of

homogeneous, heterogeneous and supported catalysts have been conducted to produce this molecule catalytically [16]. With regards to the molecular approach, in the early 1990s, J. Kizlink reported preliminary works describing the potential role of tin complexes, in particular Sn(IV) alkoxides [17–19]. In fact, as early as 1967, Bloodworth et al. highlighted the reactivity of tri-*n*-butyltin methoxide with carbon dioxide, demonstrating the facile insertion of CO₂ in the Sn-OMe bond and leading to (*n*-Bu)₃Sn(OMe)(OCO₂Me) (**1**). The authors observed, however, that the insertion does not take place with tributyltin phenoxide [20]. Later, in 1984, Blunden et al. monitored the reaction by ¹¹⁹Sn{¹H} NMR spectroscopy, in toluene at 30 °C, and showed a notable move of the chemical shift, i.e., from +95.5 ppm (*n*-Bu₃SnOMe) to –27 ppm (**1**) in the presence of CO₂ [21]. In a more recent study, D. Ballivet-Tkatchenko et al. systematically investigated the reactivity of tributyltin derivatives, *n*-Bu₃SnOR (R = Me; *i*-Pr; *t*-Bu; SnBu₃) with CO₂, observing, on the basis of the recorded values of δ¹¹⁹Sn{¹H} NMR, the presence of five-coordinate tin atoms in the carbonated species [22]. In 1999, by focusing more specifically on the evolution of the tin precursor during the methanol carbonation reaction (Scheme 1), T. Sakakura et al. elucidated the structure of Me₂Sn(OMe)₂ and its CO₂ insertion product, Me₂Sn(OMe)(OCO₂Me) (**2**), which corresponded to the first characterization by X-ray crystallography of a hemicarbonato of tin complex [23]. Compound **2** was synthesized by treating a sample of Me₂Sn(OMe)₂ with an excess of CO₂ (Scheme 2).



Scheme 2. Reaction scheme leading to compound **2**.

Single-crystals of **2** were isolated from a CO₂-saturated CH₂Cl₂-Et₂O solution at 4 °C. At the solid-state, **2** adopts a dimeric structure via two bridging methoxy groups forming a centrosymmetric Sn₂O₂ four-membered ring (Figure 1). Each tin atom of **2** is linked to a hemicarbonato ligand (methylcarbonato, –OCO₂Me), η¹-O-coordinated in the terminal position. The two Sn atoms are five-coordinated and adopt a trigonal bipyramidal (TBP) geometry. The Sn₂O₂ ring and hemicarbonato fragments are nearby coplanar. The methyl chains bound to Sn are positioned on either side of the inorganic plane.

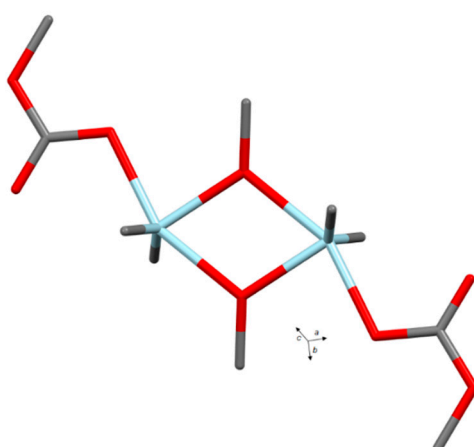
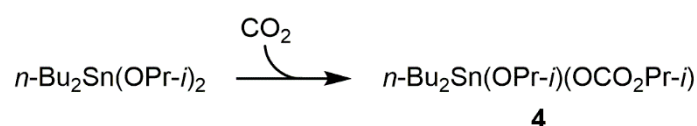


Figure 1. Molecular structure of **2**, adapted from [23] (Copyright 1999, American Chemical Society) (MERCURY view). Hydrogen atoms are omitted for clarity (Sn light blue, O red, C grey).

Analysis of **2** by IR spectroscopy corroborates the insertion of CO₂ by showing a strong vibration band at 1682 cm^{–1}. In solution in CDCl₃, at low temperature (–50 °C), the ¹¹⁹Sn{¹H} NMR spectrum of **2** displays one sharp signal at δ = –171 ppm, which is in line with pentacoordinated tin atoms,

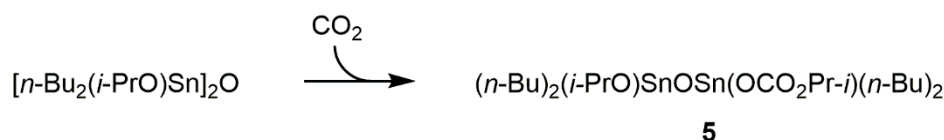
and therefore supports the preservation of the dimer structure. At room temperature, the signal becomes broader; the authors then suggest a dissociation process leading to a mononuclear complex having an intramolecularly coordinated carbonyl group [23]. Regarding the reactivity, the thermolysis of **2** (180 °C, 300 atm of CO₂) leads to the formation of DMC with a reasonable yield (58%/Sn). In parallel with this work, studying the reactivity of the di-*n*-butyl analogue, *n*-Bu₂Sn(OMe)₂ with carbon dioxide, D. Ballivet-Tkatchenko et al. acquired spectroscopic evidence of the formation of the CO₂-adduct, *n*-Bu₂Sn(OMe)(OCO₂Me) (**3**) [22,24]. When a sample of **3** was treated under vacuum at room temperature, its noncarbonated precursor was quickly recovered, demonstrating that the insertion of CO₂ is easily reversible. Although **3** was not characterized by X-ray crystallography, a comparable structure to compound **2** was proposed based on the spectroscopic data.

In 2006, using a comparable approach, D. Ballivet-Tkatchenko et al. published the reactivity of *n*-Bu₂Sn(OPr-*i*)₂ toward carbon dioxide (Scheme 3), leading to the formation of the CO₂-adduct, *n*-Bu₂Sn(OPr-*i*)(OCO₂Pr-*i*) (**4**) [25]. Again, the reaction was also found to be exothermic and reversible (under vacuum and at room temperature). The infrared spectrum of **4** shows characteristic ν(CO₃) absorption bands at 1668–1615 and 1284 cm⁻¹. Isolated as single-crystals, **4** was analyzed by X-ray crystallography, revealing a dimeric structure, showing a similar core to complex **2** [22]. Each tin atom of **4** is pentacoordinated and bears in the terminal position an isopropylcarbonato group resulting from the CO₂ insertion into a Sn–OPr-*i* bond. The authors mentioned a weak interaction between carbonyl oxygen and tin atoms [Sn⋯O(C) = 2.9114(12) Å]. A slightly shorter distance was also measured in the case of **2** [Sn⋯O(C) = 2.822 Å].



Scheme 3. Reaction scheme leading to compound **4**.

As part of this same study [25], the authors also considered the reactivity of a distannoxane species, [*n*-Bu₂(*i*-PrO)Sn]₂O toward carbon dioxide (Scheme 4).



Scheme 4. Reaction scheme leading to compound **5**.

Again, great reactivity was observed and the carbonation was also reported as being reversible, on condition that the sample be kept under vacuum overnight. The CO₂ insertion was monitored by infrared spectroscopy showing **5** characteristic ν(CO₃) absorption bands at 1647–1627 and 1286 cm⁻¹. Recrystallization in diethylether at 4 °C promoted the growth of suitable single-crystals, finally characterized as (*n*-Bu)₂(*i*-PrO)SnOSn(OCO₂Pr-*i*)(*n*-Bu)₂ (**5**). The X-ray crystallographic structure of **5** was described as a centrosymmetric dimeric structure with a built-in ladder-type arrangement exhibiting two distinct tin centers in the exo- and endo- cyclic positions. Again, as with **4**, the insertion of CO₂ into the Sn–OPr-*i* bond resulted in the formation of two isopropylcarbonato groups, η¹-O-coordinated to Sn, and exclusively located on the two exocyclic tin atoms (Figure 2). All tin atoms of **5** are pentacoordinated in a distorted trigonal bipyramid (TBP) and are linked via oxygen atoms according to a zigzag arrangement, as commonly observed for distannoxanes [26].

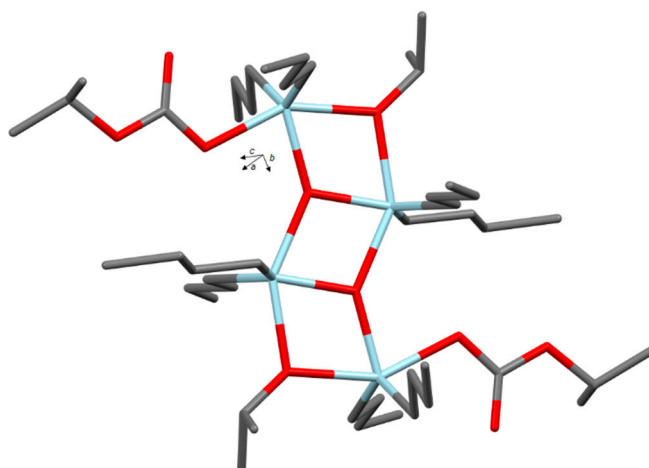
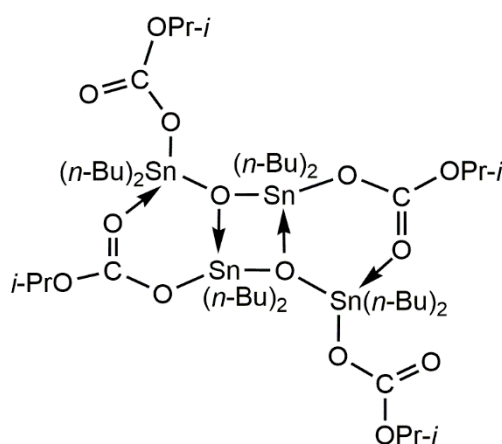


Figure 2. Molecular structure of **5**, adapted from [25] (Copyright 2006, Royal Society of Chemistry) (MERCURY view). Hydrogen atoms are omitted for clarity (Sn light blue, O red, C grey).

Recently, on the basis of NMR spectroscopy experiments at high pressure, carried out under 50 bar of CO₂ pressure at 80 °C, either in isopropanol-*d*₈ or toluene-*d*₈, the existence of a species with four isopropylcarbonate groups and arising from **5** was also suggested [27] (Scheme 5). Thus, compound **6**, formulated as $\{[n\text{-Bu}_2\text{Sn}(\text{OCO}_2\text{Pr-}i)_2]\text{O}_2\}_2$, would result from the additional reactivity of **5** via the insertion of CO₂ into the two remaining noncarbonated isopropoxy ligands. However, to date, the existence in the solid-state of such a tetracarboxylated distannoxane complex remains to be confirmed by X-ray crystallography.



Scheme 5. Molecular representation of the plausible tetrahemicarbonato distannoxane **6** resulting from the reactivity of **5** with CO₂; adapted from [27] (Copyright 2015, Elsevier).

In the past, and still within the framework of the selective synthesis of dimethyl carbonate from CO₂ and methanol (Scheme 1), D. Ballivet-Tkatchenko et al. reported the synthesis and characterization by volumetry, multinuclear NMR and IR spectroscopies of a methylcarbonato analogue of **5**, characterized as 1-methoxy-3-methylcarbonatotetrabutyl-distannoxane, $[(n\text{-Bu})_2(\text{MeO})\text{SnOSn}(\text{OCO}_2\text{Me})(n\text{-Bu})_2]_2$ (**7**), and resulting from a 1:1 adduct with CO₂ [28]. However, the X-ray structure of **7** has not yet been resolved.

In terms of reactivity, it is accepted that distannoxane derivatives produce only traces of DMC from carbon dioxide and methanol, even under elevated conditions of temperature and pressure [28]. Moreover, monoalkoxides of triorganostannanes are known to be inactive [23]. To date, the most efficient molecular species for the DMC synthesis remains dialkoxides of diorganostannanes. Dimethyl

and di-*n*-butyl derivatives are the most studied species, and are often used as models for theoretical calculations and simulations [29–31], as well as precursors for grafting reactions on solid supports [32].

Table 1. Comparison of selected structural parameters found in hemicarbonates of organotin complexes.

Compounds	Sn–O(C) (Å)	C–O(Sn) (Å)	C=O (Å)	O–C–O (deg)	O–C=O (deg)	CSD Entry Deposition Number	Ref.
$[(\text{CH}_3)_2\text{Sn}(\text{OCH}_3)(\text{OCO}_2\text{CH}_3)]_2$ (2)	2.192(2)	1.292(4) 1.353(4)	1.201(4)	115.9(3)	125.9(3)	FATVOL 119276	[23]
$[(n\text{-Bu})_2\text{Sn}(\text{OPr-}i)(\text{OCO}_2\text{Pr-}i)]_2$ (4)	2.1696(12)	1.290(2) 1.350(2)	1.224(2)	117.27(15)	125.19(16) 117.53(16)	MEPJAT 614750	[25]
$[(n\text{-Bu})_2(i\text{-PrO})\text{SnOSn}(\text{OCO}_2\text{Pr-}i)(n\text{-Bu})_2]$ (5)	2.159(4)	1.293(6) 1.336(7)	1.233(6)	111.6(6)	125.1(5) 123.3(5)	MEPJEX 614751	[25]

Table 2. Selection of spectroscopic data (NMR and IR) assigned to hemicarbonates of tin complexes.

Compounds	$^{119}\text{Sn}\{^1\text{H}\}$ NMR (δ , ppm)	$^{13}\text{C}\{^1\text{H}\}$ NMR (δ , ppm)	IR $\nu(\text{CO}_3)$ cm^{-1}	Ref.
$(n\text{-Bu})_3\text{Sn}(\text{OMe})(\text{OCO}_2\text{Me})$ (1)	−27.0 ^a	158.4 ^b	1600	[20–22]
$[(\text{CH}_3)_2\text{Sn}(\text{OCH}_3)(\text{OCO}_2\text{CH}_3)]_2$ (2)	−170.91 ^b (s, −50 °C) −171.91 ^b (br, +25 °C)	159.19 ^b	1682	[23]
$[(n\text{-Bu})_2\text{Sn}(\text{OMe})(\text{OCO}_2\text{Me})]_2$ (3)	−213.0 ^b	156.0 ^b	1655 1303	[24]
$[(n\text{-Bu})_2\text{Sn}(\text{OPr-}i)(\text{OCO}_2\text{Pr-}i)]_2$ (4)	−209.5 ^b (br)	158.24 ^b	1668–1615 1284	[25]
$[(n\text{-Bu})_2(i\text{-PrO})\text{SnOSn}(\text{OCO}_2\text{Pr-}i)(n\text{-Bu})_2]$ (5)	−185.9 ^b −209.6 ^b	156.95 ^b	1647–1627 1286	[25]
$\{[n\text{-Bu}_2\text{Sn}(\text{OCO}_2\text{Pr-}i)_2\text{O}]_2\}$ (6)	−218.0 ^c −229.0 ^c	157.0 ^c	1678–1591	[25]
$[(n\text{-Bu})_2(\text{MeO})\text{SnOSn}(\text{OCO}_2\text{Me})(n\text{-Bu})_2]$ (7)	−176.6 ^b −208.5 ^b	157.99 ^b	1715, 1670, and 1629 1300	[28]

^a Measured in toluene-*d*₈, at 30 °C; ^b measured in CDCl₃; ^c measured in toluene-*d*₈, under CO₂ pressure (50 bar).

3. Carbonato Tin Complexes

Carbonate derivatives of organotin complexes have been discovered since the 19th century [33]. However, they have only studied more deeply since the 1960s, first by Mossbauer and infrared spectroscopy [34,35], then from the 1980s by NMR spectroscopy in solution as well as in solid-state [36]. Since then, several crystallographic determinations of carbonate tin complexes have been resolved. The X-ray structures elucidated for these compounds are listed and described below as a function of the decreasing number of alkyl ligands linked to the tin atom, i.e., from triorgano- to mono- organotin. Finally, three CO₂ derivatives of chelated stannoxanes and one of a trinuclear Sn-capped nickel cluster are also described in the last part of this chapter.

3.1. Triorganotin Derivatives

The first X-ray crystallographic analysis of such a compound was resolved in 1983 by E.R.T. Tiekink, who reported the crystal structure of bis(trimethyltin)carbonate, $(\text{Me}_3\text{Sn})_2\text{CO}_3$ (8) at room temperature [37]. A few years later, A. Sebald et al. reproduced the measurement at lower temperatures (200 K), leading to a similar structure [38]. Compound 8 was obtained by passing a stream of dry carbon dioxide through a toluene solution of trimethyltin hydroxyde. The slow evaporation at room temperature led to the growth of colorless crystals. The structure of 8 can be described as a polymeric zigzag chain consisting of SnMe₃ moieties bridged by carbonate dianions (Figure 3). Two distinct sites

of tin atoms can be observed: (i) those located in the main chain exhibit a trigonal bipyramidal geometry whose equatorial plane is occupied by three methyl substituents and the apical positions by two oxygen atoms, (ii) pendant SnMe_3 groups, connected according to a syndiotactic modes, are in a tetrahedral arrangement. The ^{119}Sn cross polarization magic-angle spinning nuclear magnetic resonance (CP MAS NMR) data support this structural feature by also showing two distinct resonances at +123.3 ppm (four-coordinate tin atom) and -62.2 ppm (five-coordinate tin atom) [38]. $(n\text{-Bu}_3\text{Sn})_2\text{CO}_3$ (**9**) could be synthesized in the same way from a solution of toluene bis(tri-*n*-butyltin) oxide by reacting with CO_2 . The $^{119}\text{Sn}\{^1\text{H}\}$ NMR spectrum showed two broad resonances ($\delta = +82$ and -66.7 ppm), suggesting a structure analogous to **8**. However, obtained as a viscous oil, to our knowledge, the solid-state structure of **9** has not yet been resolved by X-ray characterization [21]. In 1992, A. Sebald et al., in a low temperature, single crystal X-ray diffraction study, determined the structure of the isobutyl analogue, $(i\text{-Bu}_3\text{Sn})_2\text{CO}_3$ (**10**) [38]. Compound **10** crystallized in the same space group as **8** ($P2_12_12_1$) and also showed a one-dimensional, zigzag chain-like polymeric organization. However, compared to **8**, in **10** the repeating syndiotactic motif is more complex and involves two pendant $\text{Sn}(i\text{-Bu})_3$ units (Figure 4).

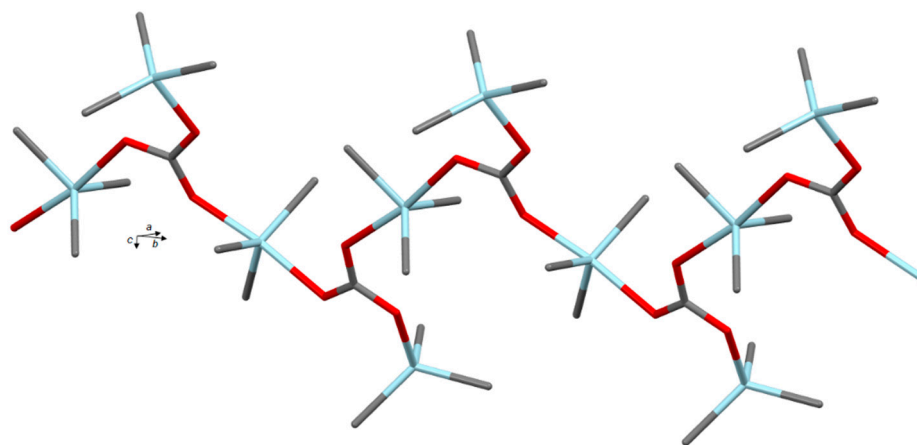


Figure 3. Molecular structure of **8**, adapted from [37,38] (Copyright 1986, Elsevier) (MERCURY view). Hydrogen atoms are omitted for clarity (Sn light blue, O red, C grey).

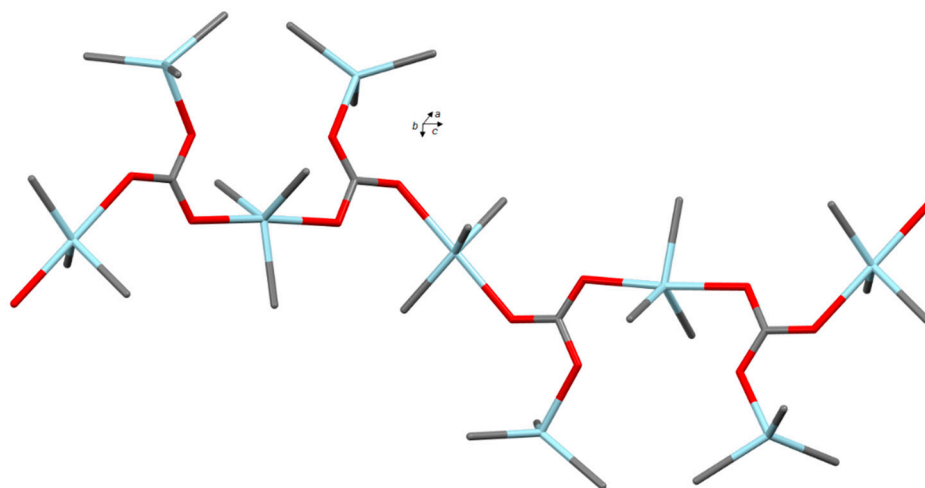
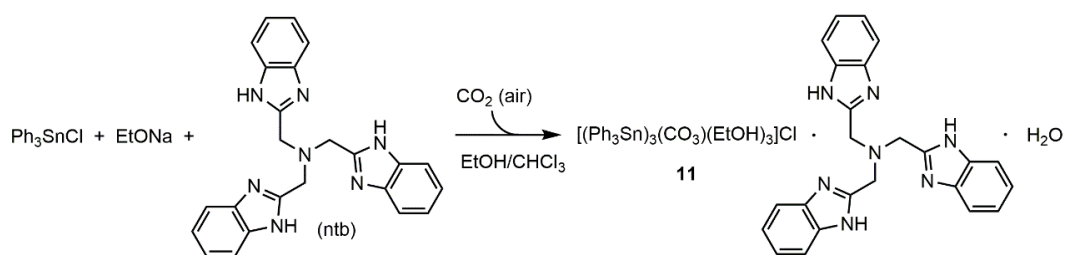


Figure 4. Molecular structure of **10**, adapted from [38] (Copyright 1992, Elsevier) (MERCURY view). Hydrogen atoms and $-\text{CH}(\text{CH}_3)_2$ groups of *i*-Bu groups are omitted for clarity (Sn light blue, O red, C grey).

Since then, three additional exemplars of triorganotin carbonates have been characterized by X-ray diffraction analysis. These compounds all result from direct atmospheric CO_2 capture. Thus,

in 2008, J.-F. Ma et al. reported the synthesis and characterization of the salt $[(\text{Ph}_3\text{Sn})_3(\text{CO}_3)(\text{EtOH})_3]\text{Cl}$ (**11**) isolated at room temperature and under ambient air, from a mixture of EtONa , Ph_3SnCl and tris(2-benzimidazolymethyl) amine (ntb) in $\text{EtOH}/\text{CHCl}_3$ (Scheme 6) [39]. Compound **11** cocrystallized with one ntb molecule and one water molecule. The structure of the cationic trinuclear cluster $[(\text{Ph}_3\text{Sn})_3(\text{CO}_3)(\text{EtOH})_3]^+$ reveals a central carbonato anion exhibiting a syn-anti μ_3 coordination mode and connecting three $(\text{EtOH})\text{Ph}_3\text{Sn}$ moieties. Sn atoms are five-coordinated in a TBP environment. The equatorial plane is occupied by three phenyl substituents and the apical positions by two oxygen atoms (Figure 5). From a supramolecular point of view, $\text{O}-\text{H}\cdots\text{N}$ hydrogen bonds involving coordinated ethanol of $[(\text{Ph}_3\text{Sn})_3(\text{CO}_3)(\text{EtOH})_3]^+$ and aromatic nitrogen atoms of ntb lead to a three-dimensional network.



Scheme 6. Reaction scheme leading to compound **11**.

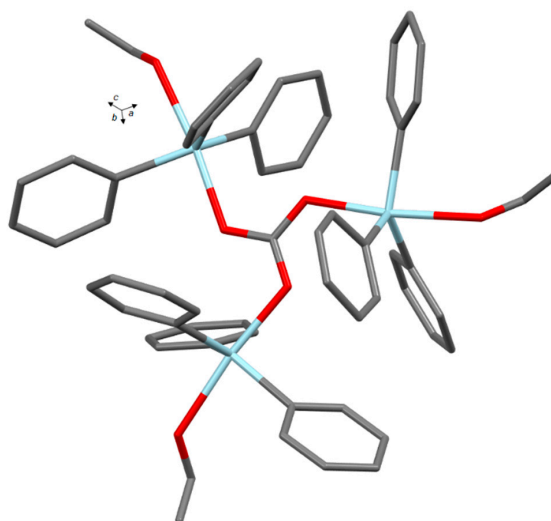


Figure 5. Molecular structure of the cation of **11**, adapted from [39] (Copyright 2008, Elsevier) (MERCURY view). Hydrogen atoms are omitted for clarity (Sn light blue, O red, C grey).

More recently, I. Haiduc and M. Andruh et al. isolated two new specimens as single crystals based on a trinuclear carbonato-centered core [40]: $[(\text{Ph}_3\text{SnCl})_2(\mu_3\text{-CO}_3)(\text{Ph}_3\text{Sn})(\text{Hbpa})]\cdot\text{H}_2\text{O}$ (**12**) and $^1_\infty[(\text{Ph}_3\text{SnCl})(\text{Ph}_3\text{Sn})_2(\mu_3\text{-CO}_3)(\text{bpa})]\cdot\text{H}_2\text{O}$ (**13**). They were obtained by reacting triphenyltin chloride with 1,2-bis(4-pyridyl)ethane (bpa) in methanol and aqueous ammonia. Only the reaction temperature differed in the synthesis protocol: at 4°C for **12**, and at room temperature for **13**. Compound **12** consists of a discrete trinuclear complex (Figure 6), while **13** is a one-dimensional coordination polymer describing a zigzag chain (Figure 7). In both cases, the carbonato group exhibits a central position, comparable to **11**, bound to three tin atoms and acting as syn-anti μ_3 -ligand. All tin atoms are five-coordinated and display a TBP geometry in which equatorial positions are occupied by phenyls groups. The authors claimed that alkaline reaction conditions (20% ammonia aqueous solution) promote the capture of atmospheric CO_2 , leading to carbonato triorganotin **12** and **13**.

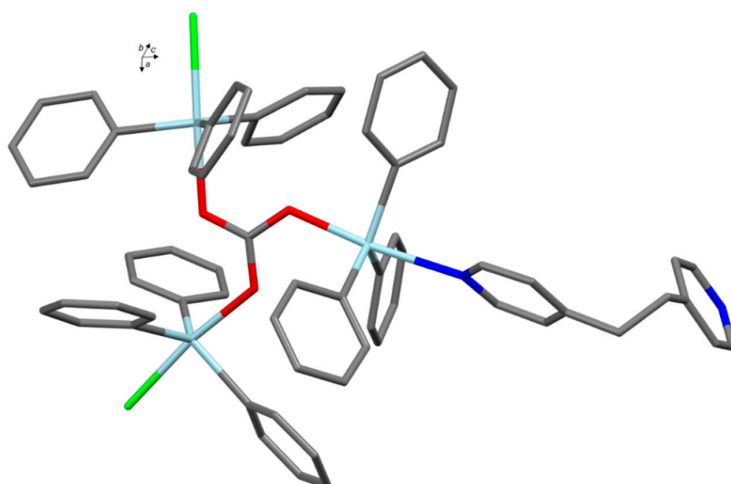


Figure 6. Molecular structure of **12**, adapted from [40] (Copyright 2015, Elsevier) (MERCURY view). Hydrogen atoms are omitted for clarity (Sn light blue, O red, N dark blue, Cl green, C grey).

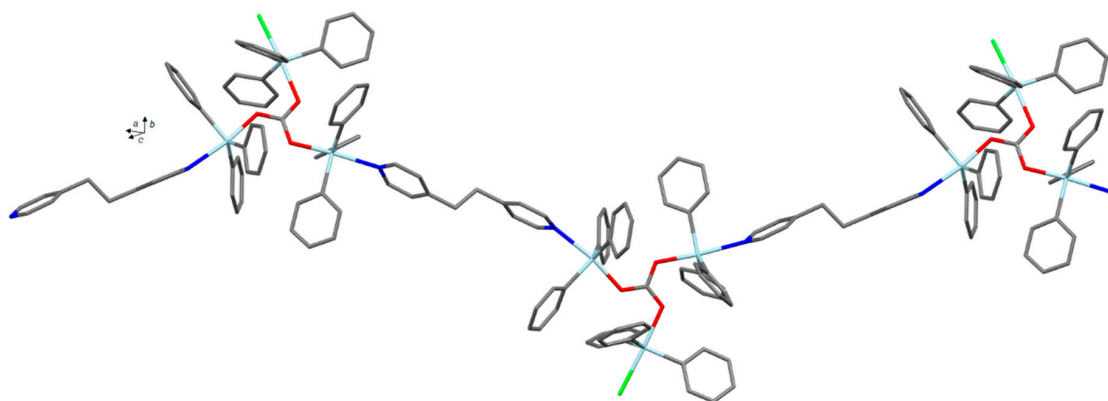


Figure 7. Molecular structure of **13**, adapted from [40] (Copyright 2015, Elsevier) [Sn light blue, O red, N dark blue, Cl green, C grey]. Hydrogen atoms are omitted for clarity (MERCURY view).

Table 3. Comparison of selected structural parameters found in carbonates of triorganotin complexes.

Compounds	Sn–O(C) (Å)	C–O (Å)	O–C–O (deg)	CSD Entry Deposition Number	Ref.
$(\text{Me}_3\text{Sn})_2\text{CO}_3$ (8)	2.247(6)	1.264(12)	118.1(8)	DOKDOW 1143774	[37]
	2.261(6)	1.267(12)	119.1(8)		
	2.031(7)	1.315(11)	122.9(8)		
$(i\text{-Bu}_3\text{Sn})_2\text{CO}_3$ (10)	2.031(5)	1.263(7)	117.4(5)	DOKDOW01 1143775	[38]
	2.258(4)	1.301(7)	120.1(5)		
	2.248(4)	1.289(7)	122.8(16)		
	2.014(12)	1.247(23)	115.4(15)		
	2.063(12)	1.227(21)	117.3(16)		
$(i\text{-Bu}_3\text{Sn})_2\text{CO}_3$ (10)	2.253(11)	1.300(22)	118.8(15)	YACKUI 1298365	[39]
	2.258(13)	1.300(23)	120.2(17)		
	2.261(12)	1.311(22)	122.5(17)		
	2.272(13)	1.321(22)	125.8(16)		
	2.164(5)	1.26(1)	120.0(8)		
$[(\text{Ph}_3\text{SnCl})_2(\mu_3\text{-CO}_3)(\text{Ph}_3\text{Sn})(\text{Hbpa})]\cdot\text{H}_2\text{O}$ (12)	2.133(5)	1.273(9)	120.3(6)	QUKMIU 1052912	[41]
	2.251(5)	1.278(8)	118.9(6)		
	2.137(5)	1.294(8)	120.9(6)		
$^1_\infty[(\text{Ph}_3\text{SnCl})(\text{Ph}_3\text{Sn})_2(\mu_3\text{-CO}_3)(\text{bpa})]\cdot\text{H}_2\text{O}$ (13)	2.142(3)	1.277(6)	120.0(5)	QUKMOA 1052913	[42]
	2.234(4)	1.277(7)	119.6(5)		
	2.135(3)	1.289(7)	120.5(5)		

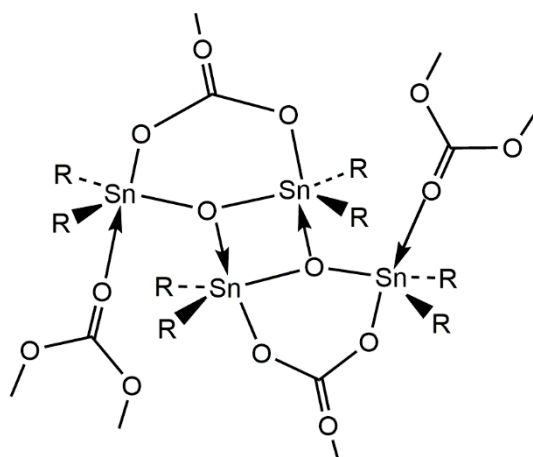
Table 4. Selection of spectroscopic data (NMR and IR) assigned to carbonates of triorganotin complexes.

Compounds	$^{119}\text{Sn}\{^1\text{H}\}$ NMR (δ , ppm)	^{119}Sn MAS NMR (δ_{iso} , ppm)	$^{13}\text{C}\{^1\text{H}\}$ NMR (δ , ppm)	^{13}C MAS NMR (δ_{iso} ppm)	IR $\nu(\text{CO}_3)$ cm^{-1}	Ref.
(Me_3Sn) $_2\text{CO}_3$ (8)	n/a	+123.5 −62.2	n/a	163.8	1553, 1534 1379, 1072	[35,38]
(<i>n</i> - Bu_3Sn) $_2\text{CO}_3$ (9)	+82.0 ^a −66.7 ^a	n/a	n/a	n/a	n/a	[21]
(<i>i</i> - Bu_3Sn) $_2\text{CO}_3$ (10)	+101.7 ^b	+86.5 −75.1 −96.4	162.2 ^b	163.3	n/a	[38]
[(Ph_3Sn) $_3(\text{CO}_3)(\text{EtOH})_3$](<i>ntb</i>)-Cl·H $_2\text{O}$ (11)	n/a	n/a	n/a	n/a	1455	[39]
[(Ph_3SnCl) $_2(\mu_3\text{-CO}_3)(\text{Ph}_3\text{Sn})(\text{Hbpa})$]-H $_2\text{O}$ (12)	n/a	n/a	n/a	n/a	1428 829	[40]
$^1_\infty$ [(Ph_3SnCl)(Ph_3Sn) $_2(\mu_3\text{-CO}_3)(\text{bpa})$]-H $_2\text{O}$ (13)	n/a	n/a	n/a	n/a	1428 896	[40]

^a Measured in toluene, at 30 °C; ^b measured in CDCl $_3$.

3.2. Diorganotin Derivatives

Carbonato derivatives of diorganotins also aroused great interest in the 70s and 80s. In 1976, R. G. Goel et al. published a synthesis and spectroscopic characterization of (Me_2Sn) $_2\text{O}(\text{CO}_3)$ by reacting an aqueous solution of potassium carbonate with an acetone solution of dimethyltin dichloride [41]. Similarly, (PhSn) $_2\text{O}(\text{CO}_3)$ was prepared from cesium carbonate and diphenyltin dichloride in methanol solution at ambient temperature. Mainly based on ^{119}Sn Mössbauer and infrared spectroscopic data, a polymeric oxycarbonate structure was suggested for these compounds (Scheme 7). Some years later, P. J. Smith et al. extended this work by publishing the spectroscopic data of new dialkyltin derivatives (R = Et, Pr, Bu, Oct), still suggesting a network organization based on Goel's model [42]. The structure is supposed to contain intermolecularly bridging carbonate groups, as well as four-membered Sn $_2\text{O}_2$ rings.



Scheme 7. Goel's model proposed for diorganotin oxycarbonates, adapted from [41,42] (Copyright 1983, Elsevier).

Regarding X-ray crystallographic structures, diorganotin derivatives are the most represented carbonato tin complexes in CSD. To our knowledge, up to now, twelve depositions have been reported, corresponding to ten distinct compounds. The first structure of such a compound was reported in 1997 by R. Borsdorf et al. for [(*n*- Bu_2Sn -Pyr) $_2(\text{CO}_3)$] (14) [43]. Compound 14 was isolated as orange crystals from the reaction in methanol involving an equimolar mixture of *n*- Bu_2SnO and methyl 2-pyridylmethylidenehydrazinecarbodithioate (HPyr), and in the presence of NaHCO $_3$. CO $_3^{2-}$ is coordinated to two tin atoms according to a $\mu_2\text{-}\kappa^2\text{:}\eta^1$ coordination mode (Figure 8). The tin atoms

present two distinct environments. One can be considered heptacoordinated with, in particular, a bond of 2.506(6) Å between carbonyl oxygen and tin atom, and the second pentacoordinated, although Sn–O and Sn–N interactions measuring 2.826(6) and 2.777(7) Å, respectively, exist (Figure 8).

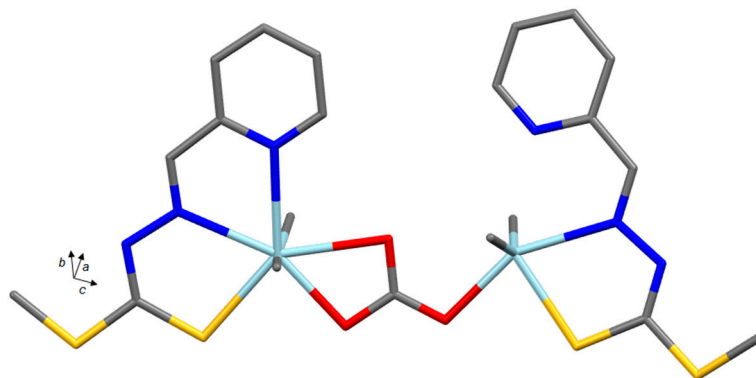


Figure 8. Molecular structure of **14**, adapted from [43] (Copyright 1997, WILEY-VCH VERLAG GMBH & CO. KGAA) (MERCURY view). Hydrogen atoms are omitted for clarity and for each *n*-butyl chain; only the α -carbon atoms bonded to tin are shown (Sn light blue, O red, N dark blue, S yellow, C grey).

Several carbonate derivatives of organooxotin clusters have also been isolated and characterized in the solid-state. It has been known for a long time that organooxotin clusters assembled by Sn–O bonds lead to a rich diversity of architectures with variable nuclearities (from discrete mononuclear compounds to complex clusters and multidimensional networks). Several review articles have been dedicated to their astonishing topologies [44,45]. Regarding the class of carbonates, the most common structure recorded for diorganotin derivatives consists of a raft-like arrangement based on two almost planar Sn_5O_5 ladders, and connected by two carbonato ligands. All tin atoms display a TBP geometry, and bear two alkyl ligands in equatorial positions. To our knowledge, four X-ray depositions of this type of compound have been identified to date. The first example, $[(\text{R}_2\text{SnO})_3(\text{R}_2\text{SnOH})_2(\text{CO}_3)]_2$ (**15**) ($\text{R} = -\text{CH}_2\text{C}_6\text{H}_5$), was isolated by J.-F. Ma et al., studying the hydrolysis of dibenzyltin dichloride in ethanol in the presence of atmospheric CO_2 [46]. Compound **15** can also be synthesized and characterized as toluene solvate by reacting dibenzyltin oxide with dimethyl carbonate in the presence of toluene and methanol [47]. Meanwhile, for compound **15**, the four corners of the inorganic framework are occupied by four bridging hydroxyl groups by changing the reaction conditions (and addition of hypnone). J.-F. Ma et al. succeeded in isolating an ethanolate-modified cluster $[(\text{R}_2\text{SnO})_3(\text{R}_2\text{SnOH})(\text{R}_2\text{SnOC}_2\text{H}_5)(\text{CO}_3)]_2$ ($\text{R} = -\text{CH}_2\text{C}_6\text{H}_5$) (**16**). In **16**, two diagonally opposite hydroxyl groups were replaced by two ethanolate groups. Later, a decanuclear cluster in which the four μ -OH groups were substituted was obtained in 2006 by D. Ballivet-Tkatchenko et al. explored the direct synthesis of dimethyl carbonate from CO_2 and methanol (Scheme 1), $\text{R} = -\text{CH}_3$) in the presence of di-*n*-butyldimethoxystannane. During experiments of recycling, i.e., by repeating catalytic runs under 200 bar of CO_2 at 150 °C, single-crystals of $[(n\text{-Bu}_2\text{SnO})_3(n\text{-Bu}_2\text{SnOCH}_3)_2(\text{CO}_3)]_2$ (**17**) were grown from a methanol solution at room temperature [48]. Thus, the four corners of **17** are occupied by four methoxy bridging groups (Figure 9). Their presence was suspected to be directly related to the formation of DMC. In addition, and during recycling runs carried out in the presence of 2,2-dimethoxypropane (usually used as dehydrating agent), S. R. Sanapureddy and L. Plasseraud also suspected the existence of a close relationship between $[(n\text{-Bu}_2\text{SnO})_3(n\text{-Bu}_2\text{SnOCH}_3)_2(\text{CO}_3)]_2$ (**17**) and the oxycarbonate, $(n\text{-Bu}_2\text{Sn})_2\text{O}(\text{CO}_3)$ [49].

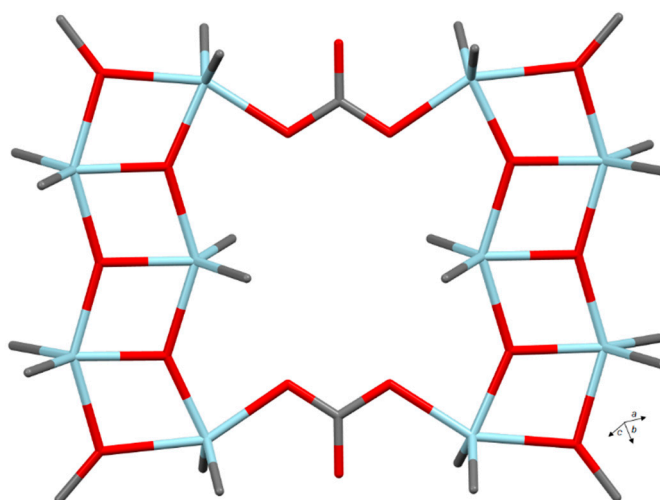


Figure 9. Molecular structure of **17**, highlighting the occupation of the four corners by $-\text{OCH}_3$ ligands, adapted from [48] (Copyright 2006, Elsevier) (MERCURY view). Hydrogen atoms are omitted for clarity and for each *n*-butyl chain; only the α -carbon atoms bonded to tin are shown (Sn light blue, O red, C grey).

Subsequently, L. Plasseraud and R. Willem et al. published two alternative synthetic routes leading to compound **17**: (i) from di-*n*-butyltin oxide, in a sealed vial and in the presence of DMC, (ii) from a chlorinated organotin complex $n\text{-Bu}_2\text{Sn}(\text{OCH}_3)\text{Cl}$, generated in situ from $n\text{-Bu}_2\text{Sn}(\text{OCH}_3)_2$ and $n\text{-Bu}_2\text{SnCl}_2$, and in the presence of K_2CO_3 . An ethoxy analogue of **17**, $[(n\text{-Bu}_2\text{SnO})_3(n\text{-Bu}_2\text{SnOC}_2\text{H}_5)_2(\text{CO}_3)]_2$ (**18**), was also synthesized by applying the sealed vial method and using diethyl carbonate as reactant. Moreover, **17** and **18** were fully characterized in solution by 1D NMR investigations, as well as by ^1H - ^{119}Sn 2D heteronuclear correlation spectroscopy experiments [50]. Remarkably, these decanuclear species displaying raft-like structures are characterized in solution by three $^{119}\text{Sn}\{^1\text{H}\}$ resonances exhibiting a 1:2:2 intensity ratio, in full agreement with X-ray structures. For **17**, a comparable fingerprint was recorded at the solid-state.

By changing the nature of the two alkyl ligands linked to tin, a different framework was achieved. Thus, when a di-*tert*-butyltin oxide suspension in methanol is treated with an aqueous solution of Na_2CO_3 , it results in the formation of needle-like crystals characterized as $[(t\text{-Bu}_2\text{Sn})_3\text{O}(\text{OH})_2]\text{CO}_3 \cdot 3\text{MeOH}$ (**19**) [51]. The use of acetone instead of methanol during the synthesis leads to an analogous complex, crystallizing with three molecules of water and one of acetone, $[(t\text{-Bu}_2\text{Sn})_3\text{O}(\text{OH})_2]\text{CO}_3 \cdot 3\text{H}_2\text{O} \cdot \text{acetone}$ (**20**). Complex **19** was also isolated by D. Ballivet-Tkatchenko et al. during the study of the reactivity of di-*tert*-butyldimethoxystannane for the synthesis of dimethyl carbonate from carbon dioxide and methanol [52]. The skeleton of **19** and **20** consists of an almost planar Sn_3O_3 core. The two outer tin atoms are linked to a carbonate ligand acting as a bidentate chelating ligand according to a syn-syn coordination mode. The three tin atoms are pentacoordinated in a distorted TBP arrangement. They are connected to two *tert*-butyl ligands located in the equatorial plane, and their coordination sphere is completed by three oxygen atoms, coming from $\mu_3\text{-O}$, $\mu\text{-OH}$ or $\mu\text{-CO}_3$ ligands (Figure 10). H. Reuter and H. Wilberts also qualified this type of topology as a butterfly structure resulting from two four-membered tin-oxygen rings, fused together [51]. In solution, although very slightly soluble, these compounds were characterized by a pair of $^{119}\text{Sn}\{^1\text{H}\}$ resonances (1:2 ratio) corresponding to two pentacoordinate tin environments [52].

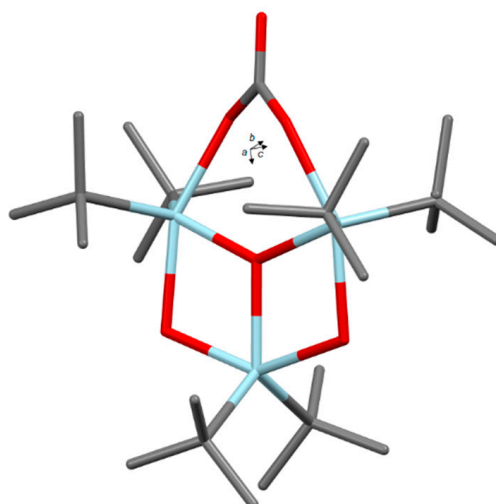


Figure 10. Molecular structure of **19** and **20**, adapted from [51,52] (Copyright 2006, Elsevier) (MERCURY view). Hydrogen atoms and solvent molecules are omitted for clarity (Sn light blue, O red, C grey).

Interestingly, the trinuclear framework described above was subsequently isolated as building-blocks in more complex skeletons of organooxotins. Firstly, in 2010, J. Beckmann et al. reported the multinuclear hypercoordinated organostannoxane carbonate cluster $[t\text{-Bu}_2\text{Sn}(\text{OH})\text{OSnR}(\text{OH})_2\text{OC}(\text{OSn}t\text{-Bu}_2\text{OH})_2(\text{O})\text{SnR}(\text{OH})(\text{H}_2\text{O})]_2$ ($\text{R} = 2,6\text{-Mes}_2\text{C}_6\text{H}_3$) (**21**) [53]. Compound **21** was prepared by purging with an excess of CO_2 a mixture of *trans*- $[2,6\text{-Mes}_2\text{C}_6\text{H}_3\text{Sn}(\text{O})(\text{OH})]_3$ and (*t*- Bu_2SnO) in THF. The authors described the unusual structure of **21** as the assembly of two trinuclear $\text{OC}(\text{OSn}t\text{-Bu}_2)_2\text{O}-(2,6\text{-Mes}_2\text{C}_6\text{H}_3)\text{Sn}(\text{OH})_2$ moieties connected to a central four-membered (*t*- Bu_2SnOH) $_2$ ring via two $(2,6\text{-Mes}_2\text{C}_6\text{H}_3)(\text{OH})\text{Sn}(\text{OH})_2$ units (Figure 11).

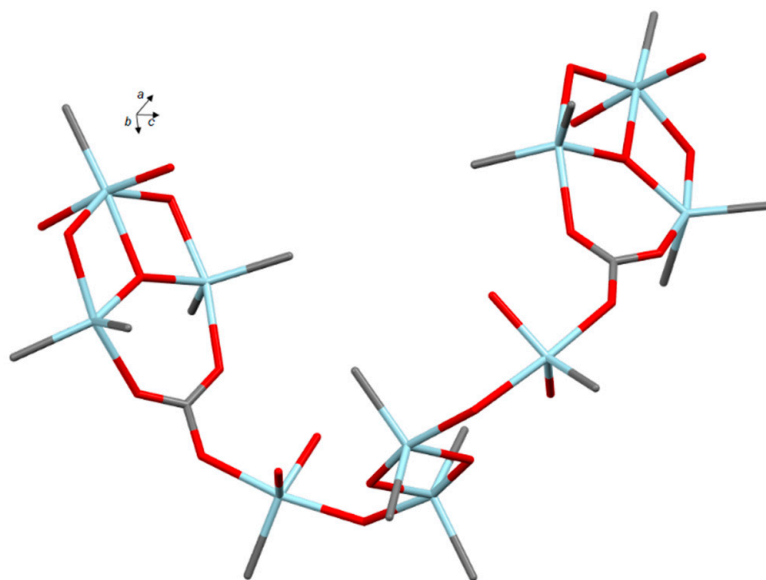


Figure 11. Molecular structure of **21**, adapted from [53] (Copyright 2010, WILEY-VCH VERLAG GMBH & CO. KGAA) (MERCURY view). Hydrogen atoms are omitted for clarity and for each R and *t*-Bu substituent, only the α -carbon atom bonded to tin is shown (Sn light blue, O red, C grey).

Recently, P. Svec and L. Plasseraud et al., studying the reactivity of $[L^{CN}(n\text{-Bu})_2\text{Sn}]^+[\text{CB}_{11}\text{H}_{12}]^-$ ($L^{CN} = 2\text{-}(N,N\text{-dimethylaminomethyl})\text{phenyl}$) for the synthesis of DMC from CO_2 and methanol, isolated a new carbonate of organostannane with a decanuclear structure and characterized it as $[(n\text{-Bu})_{20}\text{Sn}_{10}\text{O}_2(\text{OMe})_6(\text{CO}_3)_2]^{2+} \cdot 2[\text{CB}_{11}\text{H}_{12}]^-$ (**22**) [54]. The core of **22** can be described as consisting of a central tetranuclear fragment of the distannoxane type, with a characteristic ladder structure, linked by two carbonato ligands (syn-syn μ_3) to two trinuclear fragments (Figure 12). Highly soluble in THF, **22** was also fully characterized by NMR spectroscopy.

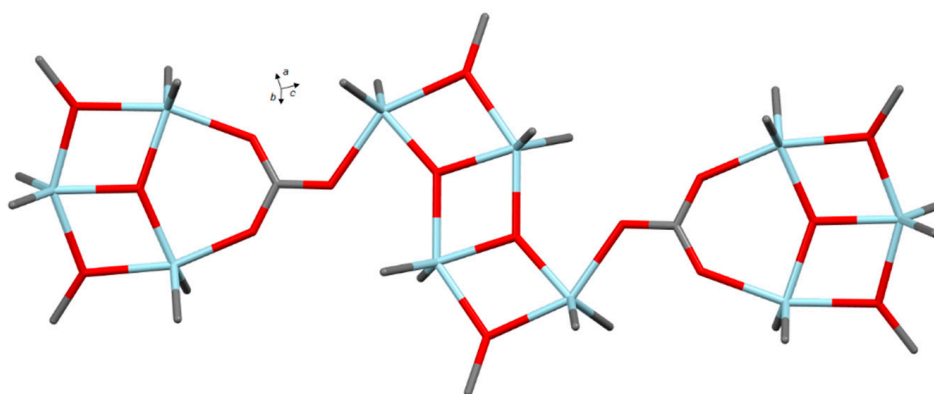
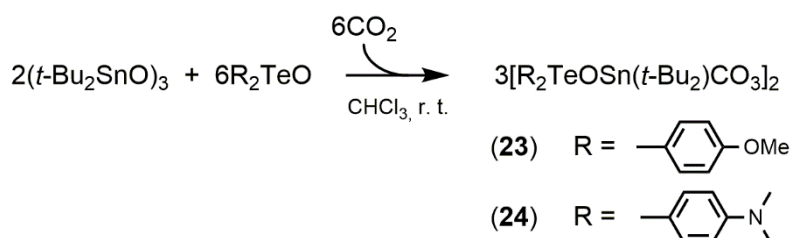


Figure 12. Molecular structure of **22**, adapted from [54] (Copyright 2018, *The Royal Society of Chemistry* and *The Centre National de la Recherche Scientifique*) (MERCURY view). Hydrogen atoms are omitted for clarity and for each *n*-butyl chain; only the carbon atom bonded to tin is shown (Sn light blue, O red, C grey).

Finally, by purging a mixture of di-*tert*-butyltin oxide and di-*p*-anisyltellurium oxide in solution in chloroform with carbon dioxide (for 15 min and at room temperature) (Scheme 8), J. Beckmann et al. isolated an unprecedented tellurastannoxane framework containing two carbonate moieties, characterized as $[(p\text{-MeOC}_6\text{H}_4)_2\text{TeOSn}(t\text{-Bu}_2\text{CO}_3)_2]$ (**23**) [55]. By applying the same synthetic protocol and using $(p\text{-Me}_2\text{NC}_6\text{H}_4)_2\text{TeO}$ as tellurium precursor, the same group achieved a yield of 95%, $[(p\text{-Me}_2\text{NC}_6\text{H}_4)_2\text{TeOSn}(t\text{-Bu}_2\text{CO}_3)_2]$ (**24**), which constitutes another example of a tellurastannoxane carbonate cluster [56]. Compounds **23** and **24** exhibit a comparable inorganic skeleton which consists of an almost planar $\text{Sn}_2\text{Te}_2\text{C}_2\text{O}_8$ core. In both cases, the Sn atoms adopt a TBP geometry and the Te atoms are considered to be hexacoordinated in octahedral environments via the presence of intramolecular $\text{Te}\cdots\text{O}$ contacts (involving oxygen atoms of carbonate moieties). The coordination mode of carbonates can be defined as $\mu_2\text{-}\kappa^2\text{:}\eta^1$, i.e., as monodentate ligand of a tellurium atom and chelating a tin atom (Figures 13 and 14).



Scheme 8. Reaction scheme leading to compounds **23** and **24**.

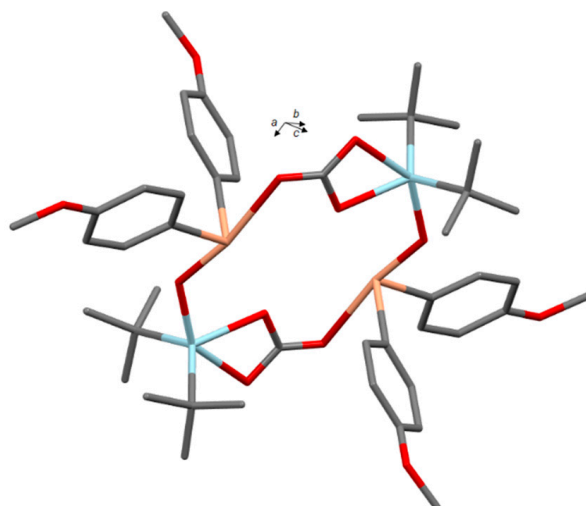


Figure 13. Molecular structure of **23**, adapted from [55] (Copyright 2004, WILEY-VCH VERLAG GMBH & CO. KGAA) (MERCURY view). Hydrogen atoms are omitted for clarity (Sn light blue, Te apricot, O red, C grey).

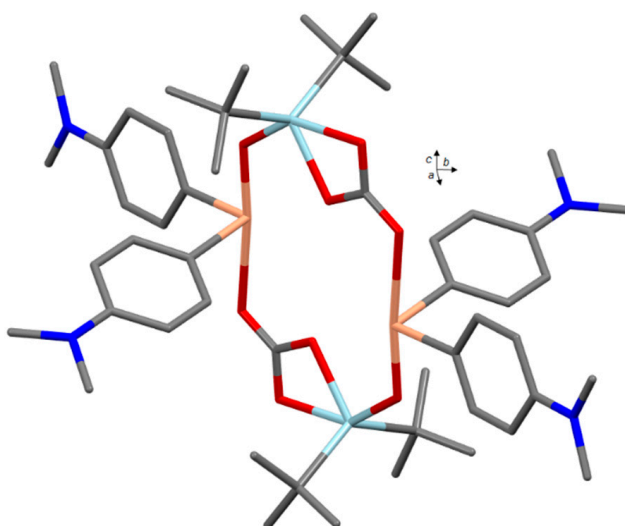


Figure 14. Molecular structure of **24**, adapted from [56] (Copyright 2004, International Union of Crystallography) (MERCURY view). Hydrogen atoms are omitted for clarity (Sn light blue, Te apricot, N dark blue, O red, C grey).

Table 5. Comparison of selected structural parameters found in carbonates of diorganotin complexes.

Compounds	Sn–O(C) (Å)	C–O (Å)	C=O (Å)	O–C–O (°)	O–C=O (deg)	CSD Entry Deposition Number	Ref.
$[(n\text{-Bu}_2\text{Sn-Pyr})_2(\text{CO}_3)]$ (14)	2.506(6) 2.229(7) 2.195(6)	1.326(11) 1.284(11)	1.260(11)	118.4(9)	122.9(9) 118.7(9)	RACXIC 106460	[43]
$[(\text{R}_2\text{SnO})_3(\text{R}_2\text{SnOH})_2(\text{CO}_3)]_2$ (15) (R = $-\text{CH}_2\text{C}_6\text{H}_5$)	2.094(2) 2.113(2)	1.304(4) 1.315(4)	1.237(4)	114.5(3)	125.5(3) 122.0(3)	MADDOL 232628 MAHQIX 763719	[46] [47]
$[(\text{R}_2\text{SnO})_3(\text{R}_2\text{SnOH})(\text{R}_2\text{SnOC}_2\text{H}_5)(\text{CO}_3)]_2$ (16) (R = $-\text{CH}_2\text{C}_6\text{H}_5$)	2.095(4) 2.116(4)	1.298(7) 1.302(7)	1.240(8)	116.4(6)	121.8(6) 121.8(6)	MADFUT 232628	[46]
$[(\text{R}_2\text{SnO})_3(\text{R}_2\text{SnOCH}_3)_2(\text{CO}_3)]_2$ (17) (R = $-n\text{-Bu}$)	2.111(6) 2.110(6)	1.291(11) 1.277(10)	1.243(10)	115.0(7)	123.2(8) 121.6(8)	DIFLAG 1140489	[48]
$[(t\text{-Bu}_2\text{Sn})_3\text{O}(\text{OH})_2]\text{CO}_3 \cdot 3\text{MeOH}$ (19)	2.140(4) 2.119(4)	1.280(7) 1.310(7)	1.266(7)	120.6(7)	120.3(6) 119.0(5)	JELZAC 278211 JELZAC01 968891	[51] [52]
$[(t\text{-Bu}_2\text{Sn})_3\text{O}(\text{OH})_2]\text{CO}_3 \cdot 3\text{H}_2\text{O} \cdot \text{acetone}$ (20)	2.125(2) 2.128(2)	1.295(3) 1.295(3)	1.250(3)	120.0(2)	120.0(2) 120.0(2)	YONZOS 968892	[51]
$[t\text{-Bu}_2\text{Sn}(\text{OH})\text{OSnR}(\text{OH})_2\text{OC}(\text{OSn}t\text{-Bu}_2\text{OH})_2(\text{O})\text{SnR}(\text{OH})(\text{H}_2\text{O})_2]$ (21)	2.11(1) 2.18(1) 2.270(9)	1.25(2) 1.27(2) 1.28(2)		117(1) 119(1) 124(1)		SUMXUU 749950	[53]
$[(n\text{-Bu})_{20}\text{Sn}_{10}\text{O}_2(\text{OMe})_6(\text{CO}_3)_2]^{2+} \cdot 2[\text{CB}_{11}\text{H}_{12}]^-$ (22)	2.11(1) 2.158(9) 2.18(1)	1.24(2) 1.29(2) 1.28(2)		125(1) 121(1) 115(1)		TEWXUR 1590299	[54]
$[(p\text{-MeOC}_6\text{H}_4)_2\text{TeOSn}(t\text{-Bu}_2\text{CO}_3)_2]$ (23)	2.307(2) 2.094(2) 2.481(2) ^a	1.278(3) 1.329(3) 1.259(3) ^a		124.7(2) 120.9(2) 114.4(2)		FERVAA 233184	[55]
$[(p\text{-Me}_2\text{NC}_6\text{H}_4)_2\text{TeOSn}(t\text{-Bu}_2\text{CO}_3)_2]$ (24)	2.313(3) 2.085(3)	1.282(6) 1.326(6) 1.252(6) ^a		123.7(5) 122.0(5) 114.3(5)		GAKNOW 259086	[56]

^a C–O(Te) bond.

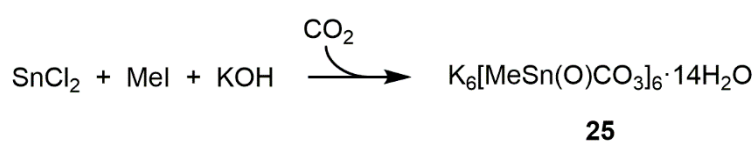
Table 6. Selection of spectroscopic data (NMR and IR) assigned to carbonates of diorganotin complexes.

Compounds	$^{119}\text{Sn}\{^1\text{H}\}$ NMR (δ , ppm)	^{119}Sn MAS NMR (δ_{iso} , ppm)	$^{13}\text{C}\{^1\text{H}\}$ NMR (δ , ppm)	^{13}C MAS NMR (δ_{iso} ppm)	IR $\nu(\text{CO}_3)$ cm^{-1}	Number Ref.
$[(n\text{-Bu}_2\text{Sn-Pyr})_2(\text{CO}_3)]$ (14)	-374.9^a	n/a	167.9^a	n/a	1420 885	[43]
$[(\text{R}_2\text{SnO})_3(\text{R}_2\text{SnOH})_2(\text{CO}_3)]_2$ (15) (R = $-\text{CH}_2\text{C}_6\text{H}_5$)	-304.7^a -244.5^a -242.6^a	n/a	164.0	n/a	1537 1363	[46,47]
$[(\text{R}_2\text{SnO})_3(\text{R}_2\text{SnOCH}_3)_2(\text{CO}_3)]_2$ (17) (R = $-n\text{-Bu}$)	-233.9^a -177.7^a -171.2^a	-235^c -181^c -174^c	163.7^a	164	1539 1373	[48,50]
$[(\text{R}_2\text{SnO})_3(\text{R}_2\text{SnOC}_2\text{H}_5)_2(\text{CO}_3)]_2$ (18) (R = $-n\text{-Bu}$)	-234^b -178^b -173^b	n/a	n/a	n/a	1535 1374	[50]
$[(t\text{-Bu}_2\text{Sn})_3\text{O}(\text{OH})_2]\text{CO}_3 \cdot 3\text{MeOH}$ (19)	-297^a -265^a	n/a	n/a	n/a	1500 (1549 ^e) 1354 (1291 ^e)	[24,52]
$[(n\text{-Bu})_{20}\text{Sn}_{10}\text{O}_2(\text{OMe})_6(\text{CO}_3)_2]^{2+} \cdot 2[\text{CB}_{11}\text{H}_{12}]^-$ (22)	-211.8^d -207.6^d -177.2^d -164.3^d	n/a	163.5	n/a		[54]
$[(p\text{-MeOC}_6\text{H}_4)_2\text{TeOSn}(t\text{-Bu}_2)\text{CO}_3]_2$ (23)	-258.3^a	-262.4	165.4^a	165.6	n/a	[55]
$[(p\text{-Me}_2\text{NC}_6\text{H}_4)_2\text{TeOSn}(t\text{-Bu}_2)\text{CO}_3]_2$ (24)	-257.9^a	-267.5	165.4^a	n/a	n/a	[56]

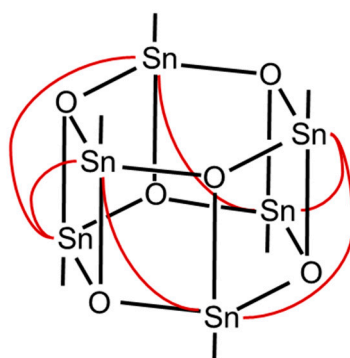
^a Measured in CDCl_3 ; ^b measured in C_6D_6 ; ^c the solid-state ^{117}Sn rather than the ^{119}Sn NMR spectrum was recorded because of local radio interferences; ^d measured in $\text{THF-}d_8$; ^e after overnight in vacuum at room temperature.

3.3. Monoorganotin Derivatives

To our knowledge, the sole example of monoorganotin carbonate characterized by an X-ray crystallographic structure was reported by J. Beckmann et al. in 2009 [57]. $K_6[MeSn(O)CO_3]_6 \cdot 14H_2O$ (**25**) was isolated from the reaction of $SnCl_2$ with methyl iodide and aqueous KOH in the presence of carbon dioxide (Scheme 9). Interestingly, the authors report that post-treatment of **25** with hot water leads to polymeric methylstannonic acid, $[MeSn(O)OH]_n$. From a structural point of view, the anionic moiety $[MeSn(O)CO_3]_6^{6-}$ exhibits a hexameric structure of prismatic type, also called drum, the two faces of which consist of two Sn_3O_6 six-membered rings bridged by six bidentate CO_3^{2-} anions, coordinated to two distinct tin atoms (Scheme 10). All tin atoms are hexacoordinated. Compound **25** was also characterized by ^{119}Sn and ^{13}C CP MAS NMR spectroscopy, showing three resonances for tin (at -474 , -481 and -486 ppm) and two sets of three signals for carbon, attributed to carbonate (at 164.2, 162.2, 160.7 ppm) and methyl groups, respectively, which was considered as being in agreement with the crystallographic structure (Table 7).



Scheme 9. Reaction scheme leading to compound **25**.



Scheme 10. Schematic representation of the drum structure of anion of **25**, adapted from [57] (Copyright 2009, American Chemical Society). The six bridging carbonate ligands are depicted by red lines.

Table 7. Selection of structural parameters found in **25**.

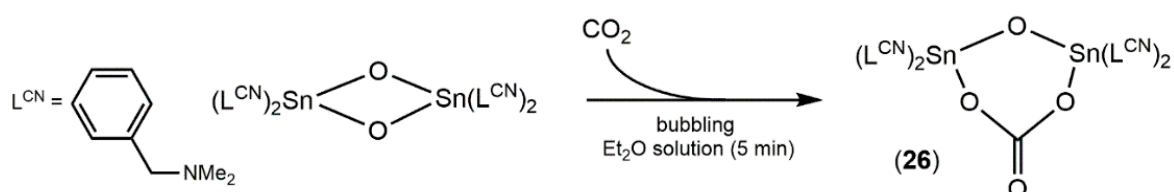
Compound	Sn–O(C) (Å)	C–O(Sn) (Å)	C=O (Å)	O–C–O (deg)	O–C=O (deg)	CSD Entry Deposition Number	Ref.
$K_6[MeSn(O)CO_3]_6 \cdot 14H_2O$ (25)	2.167(8)	1.30(1)				ZELPEN 751878	[57]
	2.129(6)	1.29(1)			120(1)		
	2.106(7)	1.32(2)	1.24(1)	121(1)	119(1)		
	2.140(8)	1.32(2)	1.24(2)	122(1)	119(1)		
	2.107(9)	1.28(2)	1.25(1)		119(1)		
		1.25(1)					
	2.122(7)	1.30(1)					

3.4. C,N-Chelated Derivatives

The first structural resolution by X-ray determination of a C,N-chelated organotin compound dates back to 1968, when Yoshida and Kasai et al. reported the crystal and molecular structure of Bis-(1,2-diethoxycarbonyl-ethyl)tin Dibromide [58]. Thereafter, this field of organotin chemistry aroused a strong interest, being firstly reviewed by J.T.B.H. Jastrzebski and G. van Koten in 1983 [59].

Nowadays, research groups of the University of Pardubice (Czech Republic) are still very active in this field, focusing on both the structural aspect and on the reactivity of *C,N*-chelated organotin [60], in particular toward carbon dioxide [61].

Thus, in 2009, A. Růžička et al. published a study devoted to the reactivity of the *C,N*-chelated stannoxane, $\{2-[(\text{CH}_3)_2\text{NCH}_2]_2\text{C}_6\text{H}_4\}_2\text{Sn}(\mu\text{-O})_2$ [62]. This compound is reported to react easily and rapidly with CO_2 in air to lead to the cyclic oxo-carbonato-bridged dinuclear complex $\{2-[(\text{CH}_3)_2\text{NCH}_2]_2\text{C}_6\text{H}_4\}_2\text{Sn}(\mu\text{-O})(\mu\text{-CO}_3)$ (**26**). A yield of 84% was also obtained for the preparation of **26** by bubbling dried CO_2 into a Et_2O solution of $\{2-[(\text{CH}_3)_2\text{NCH}_2]_2\text{C}_6\text{H}_4\}_2\text{Sn}(\mu\text{-O})_2$ (Scheme 11). According to the X-ray structure, the two tin atoms exhibit two distinct coordination geometries. One can be viewed as hexacoordinated in a distorted octahedron arrangement, and the second as pentacoordinated (TBP); the nitrogen atom of one of the two L^{CN} ligands is not bound to the tin atom (Figure 15). However, in CDCl_3 solution, the $^{119}\text{Sn}\{^1\text{H}\}$ NMR spectrum reveals only one resonance, beyond -300 ppm and slightly dependent on temperature, supporting the presence of a six-coordinate tin species. Moreover, the authors report the possible use of **26** as an active precursor for the catalytic synthesis of propylene carbonate from CO_2 and propylene oxide, with an estimated yield of 5% [62].



Scheme 11. Reaction scheme leading to compound **26**.

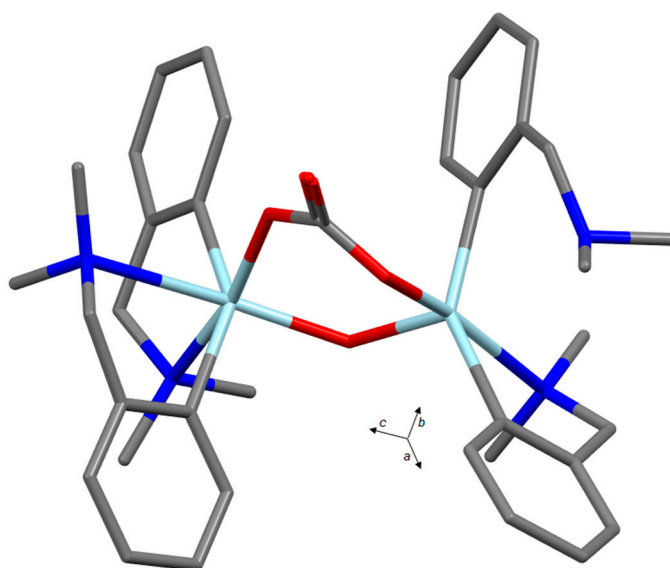
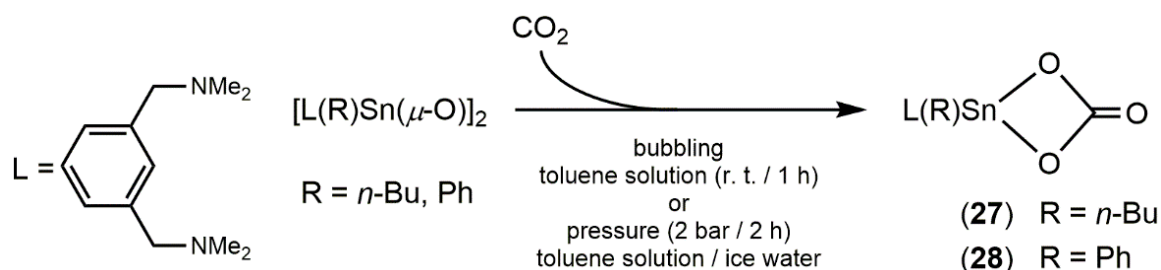


Figure 15. Molecular structure of **26**, adapted from [62] (Copyright 2009, American Chemical Society) (MERCURY view). Hydrogen atoms are omitted for clarity (Sn light blue, N dark blue, O red, C grey).

In 2012, R. Jambor and A. Růžička et al. enriched this family of carbonate derivatives by isolating two new compounds, i.e., $\text{L}(n\text{-Bu})\text{SnCO}_3$ (**27**) and $\text{L}(\text{Ph})\text{SnCO}_3$ (**28**), with $\text{L} = 2,6\text{-}(\text{Me}_2\text{NCH}_2)_2\text{C}_6\text{H}_3$ [63]. These complexes were obtained according to the same protocol of synthesis, i.e., by bubbling carbon dioxide through toluene solutions of $[\text{L}(n\text{-Bu})\text{Sn}(\mu\text{-O})]_2$ and $[\text{L}(\text{Ph})\text{Sn}(\mu\text{-O})]_2$ for one hour at room temperature (Scheme 12). Alternatively, they can also be obtained under CO_2 pressure (2 bar) by mixing dry ice with toluene solutions of organotin precursors for 2 h. Compounds **27** and **28** have been characterized by X-ray, with both presenting comparable structures (Figure 16), i.e., mononuclear complexes in which the tin atom is hexacoordinated in a strongly distorted octahedron geometry,

and *O,O*-chelated, symmetrically, by a carbonate moiety, leading to a four-membered ring (Figure 16). In CDCl₃ solution, **27** and **28**, are characterized by one ¹¹⁹Sn{¹H} NMR resonance located at δ = −379.2 and −314.0 ppm, respectively, and supporting the hexacoordination observed at the solid-state for tin atoms. In addition, the authors claimed that the CO₂ fixation by **27** and **28** was reversible, with tin precursors being quantitatively recovered by heating for 2 h under argon.



Scheme 12. Reaction scheme leading to compounds **27** and **28**.

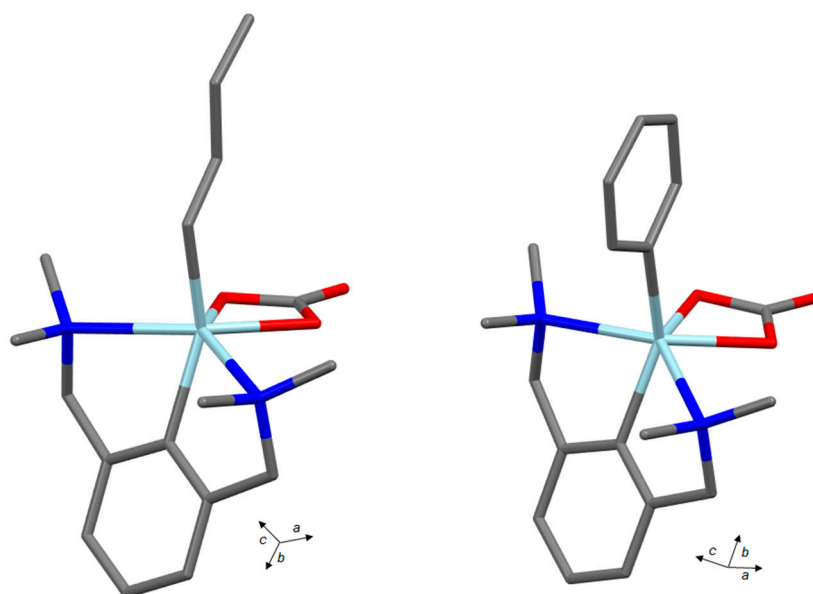


Figure 16. Molecular structure of **27** (left) and **28** (right), adapted from [63] (Copyright 2011, Elsevier) (MERCURY view). Hydrogen atoms are omitted for clarity (Sn light blue, N dark blue, O red, C grey).

Table 8. Comparison of selected structural parameters found in carbonates of *C,N*-chelated organotin complexes.

Compounds	Sn–O(C) (Å)	C–O(Sn) (Å)	C=O (Å)	O–C–O (deg)	O–C=O (deg)	CSD Entry Deposition Number	Ref.
{2-[(CH ₃) ₂ NCH ₂] ₂ C ₆ H ₄] ₂ Sn(μ-O)(μ-CO ₃) (26)	2.079(4) 2.080(4)	1.312(2) 1.322(2)	1.215(8)	116.5(5)	121.4(5) 122.1(5)	YUMVEI 119276	[62]
L(<i>n</i> -Bu)SnCO ₃ (27) (L = 2,6-(Me ₂ NCH ₂) ₂ C ₆ H ₃)	2.110(2) 2.125(2)	1.333(4) 1.325(4)	1.223(4)	111.6(3)	124.2(3) 124.2(3)	PAJMEU 835513	[63]
L(Ph)SnCO ₃ (28) (L = 2,6-(Me ₂ NCH ₂) ₂ C ₆ H ₃)	2.099(3) 2.107(3)	1.331(6) 1.322(6)	1.221(5)	110.6(4)	124.4(4) 125.0(4)	PAJMOE 835515	[63]

Table 9. Selection of spectroscopic data (NMR and IR) assigned to carbonates of C,N-chelated organotin complexes.

Compounds	$^{119}\text{Sn}\{^1\text{H}\}$ NMR (δ , ppm)	$^{13}\text{C}\{^1\text{H}\}$ NMR (δ , ppm)	IR $\nu(\text{CO}_3)$ cm^{-1}	Ref.
$\{\{2\text{-}[(\text{CH}_3)_2\text{NCH}_2]_2\text{C}_6\text{H}_4\}_2\text{Sn}(\mu\text{-O})(\mu\text{-CO}_3)\}$ (26)	−309.2 ^{a,b} −315.8 ^{a,c}	161.9 ^{d,e}	1587	[62]
L(<i>n</i>-Bu)SnCO₃ (27) (L = 2,6-(Me ₂ NCH ₂) ₂ C ₆ H ₃)	−314.0 ^{d,e}	163.9 ^{d,e}	n/a	[63]
L(Ph)SnCO₃ (28) (L = 2,6-(Me ₂ NCH ₂) ₂ C ₆ H ₃)	−379.2 ^{d,e}	163.5 ^{d,e}	n/a	[63]

^a Measured in toluene-*d*₈ or benzene-*d*₆; ^b at 350 K; ^c at 220 K; ^d measured in CDCl₃; ^e at 300 K.

3.5. Heteronuclear Cluster

Although the following compound cannot be considered an organotin derivative (no Sn-C bond), we thought it would be interesting to include it in this review. To our knowledge, this is the only example of a carbonate derivative for this family of compound.

In 2005, E. Simón-Manso and C. P. Kubiak published the reactivity of the trihydroxystannyl-capped cluster $[\text{Ni}_3(\mu\text{-dppm})_3(\mu_3\text{-Cl})(\mu_3\text{-Sn}(\text{OH})_3)]$, in solution in CH₂Cl₂ or THF, with carbon dioxide (bubbling) leading to the formation of the carbonate cluster $[\text{Ni}_3(\mu\text{-dppm})_3(\mu_3\text{-Cl})(\mu_3\text{-Sn}(\text{OH})(\eta^2\text{-CO}_3))]$ (29) [64]. The nucleophilic addition of CO₂ on the $\mu_3\text{-Sn}(\text{OH})_3$ moiety of the starting cluster causes an immediate color change, from dark blue to purple, and is accompanied by the elimination of one water molecule. The reaction is reported to be completely reversible. The Sn atom is hexacoordinated in a highly distorted octahedral coordination geometry. The coordination of the carbonate ligand to the tin atom forms a strained four-membered ring (Figure 17). By infrared, the absorption bands characteristic of carbonate are observed at 1634 and 1669 cm^{−1}. Interestingly, the authors described a comparable reactivity of the cluster $[\text{Ni}_3(\mu\text{-dppm})_3(\mu_3\text{-Cl})(\mu_3\text{-Sn}(\text{OH})_3)]$ toward 1,2-epoxybutane, leading to a 1,2-diolate tin cluster via a ring-opening addition [64].

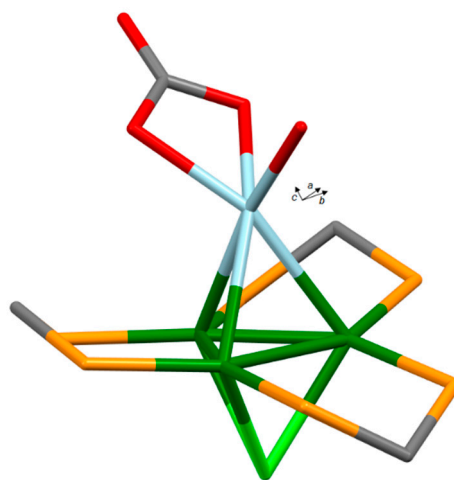


Figure 17. Molecular structure of 29, adapted from [64] (Copyright 2005, WILEY-VCH VERLAG GMBH & CO. KGAA) (MERCURY view). Hydrogen atoms and phenyl groups are omitted for clarity (Sn light blue, Ni green, P orange, Cl light green, O red, C grey).

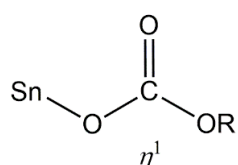
Table 10. Selection of structural parameters found in 29.

Compound	Sn–O(C) (Å)	C–O(Sn) (Å)	C=O (Å)	O–C–O (deg)	O–C=O (deg)	CSD Entry Deposition Number	Ref.
[Ni ₃ (μ-dppm) ₃ (μ ₃ -Cl)(μ ₃ -Sn(OH)(η ² -CO ₃)] (29)	2.121(3) 2.148(3)	1.325(6) 1.323(5)	1.223(6)	111.8(4)	123.9(4) 124.3(4)	FIXWEP 250077	[64]

4. Conclusions

In conclusion, this structural inventory revealed a notable number of tin compounds bearing hemicarbonato and carbonato ligands (26 CSD entries). They were discovered over a period of forty years, sometimes accidentally, but most often in the context of studies devoted to reactivity toward carbon dioxide. These compounds highlight a rich diversity of architectures, from mononuclear complex to polynuclear clusters, showing various modes of coordination (summarized in Scheme 13). From a structural point of view, the tin atom preferentially adopts a trigonal bipyramidal or an octahedral geometry. When available, spectroscopic data rather correctly corroborate the resolved structures, even for the most complex, and show that in most cases, they are kept intact in solution. In general, the formation of hemicarbonato tin complexes results from the facile insertion of carbon dioxide at atmospheric pressure into Sn–OR bonds. Their formation has been intimately linked to the direct carbonation reaction of alcohols. Organotin compounds are thus recognized as the most efficient molecular precursors for the transformation of carbon dioxide into linear alkyl carbonates. With regards to carbonato tin complexes, the majority were obtained by directly reacting an organometallic tin precursor (very often an oxide derivative) with carbon dioxide. Alternatively, in some cases, inorganic carbonate salts were also used. This last class of compounds is the most abundant and varied from a structural point of view. However, several factors are decisive for the structure of the final edifice, in particular the reaction conditions and the number and nature of the ligands linked to the tin atom. In view of the diversity of the resolved structures and their relatively small number, the combination of these parameters still provides important perspectives in terms of the synthesis and design of new compounds. Finally, it appears that organotins exhibit a high reactivity with carbon dioxide, leading to its fixation, or even conversion. Thus, the CO₂ derivatives of molecular compounds of tin can truly be considered as a class of compounds in their own right. As mentioned at the beginning of this article, other types of CO₂-adducts of tin complexes are known, such as carbamates, formates, and phosphinoformates. These derivatives can also result from the insertion of CO₂ into Sn–X bonds (X = N, H, P), and they will be the subject of a future structural inventory.

Hemicarbonato tin complexes



Compounds	CSD refcodes
(2)	FATVOL
(4)	MEPJAT
(5)	MEPJEX

Carbonato tin complexes

Compounds	CSD refcodes	Compounds	CSD refcodes
	(8) (10) (11) (12) (13)	DOKDOW YACKUI TIWROH QUKMIU QUKMOA	(14) RACXIC
	(15) (16) (17)	MADDOL MAHQIX MADFUT DIFLAG	(19) (20) (25) (26) YONZOS JELZAC ZELPEN YUMVEI
	(21) (22)	SUMXUU TEWXUR	(23) (24) FERVA GAKNOW
	(27) (28) (29)	PAJMEU PAJMOE FIXWEP	

Scheme 13. Summary of the coordination modes observed for hemicarbonato and carbonato tin complexes and described in this review (based on X-ray crystallographic structures).

Funding: L.P. thanks the Centre National de la Recherche Scientifique (C.N.R.S-France) and the University of Bourgogne Franche-Comté for financial support.

Conflicts of Interest: The author declares no conflict of interest.

References

1. Vol'pin, M.E.; Kolomnikov, I.S.; Lobeeva, T.S. Rhodium complex of carbon dioxide. *Izv. Akad. Nauk SSSR Ser. Khim.* **1969**, *2084*. [[CrossRef](#)]
2. Aresta, M.; Nobile, C.F.; Albano, V.G.; Forni, E.; Manassero, M. New nickel-carbon dioxide complex. Synthesis, properties, and crystallographic characterization of (carbon dioxide)bis(tricyclohexylphosphine)nickel. *J. Chem. Soc. Chem. Commun.* **1975**, 636–637. [[CrossRef](#)]
3. Gibson, D.H. The organometallic chemistry of carbon dioxide. *Chem. Rev.* **1996**, *96*, 2063–2095. [[CrossRef](#)] [[PubMed](#)]
4. Mascetti, J. Carbon dioxide coordination chemistry and reactivity of coordinated CO₂. In *Carbon Dioxide as Chemical Feedstock*; Aresta, M., Ed.; Wiley-VCH Verlag GmbH & Co. KGaA: Weinheim, Germany, 2010; pp. 55–88.
5. Paparo, A.; Okuda, J. Carbon dioxide complexes: Bonding modes and synthetic methods. *Coord. Chem. Rev.* **2017**, *334*, 136–149. [[CrossRef](#)]
6. Looney, A.; Han, R.; McNeill, K.; Parkin, G. Tris(pyrazolyl)hydroboratozinc hydroxide complexes as functional models for carbonic anhydrase: On the nature of the bicarbonate intermediate. *J. Am. Chem. Soc.* **1993**, *115*, 4690–4697. [[CrossRef](#)]
7. Wang, H.; Gao, P.; Zhao, T.; Wei, W.; Sun, Y. Recent advances in the catalytic conversion of CO₂ to value added compounds. *Sci. China Chem.* **2015**, *58*, 79–92. [[CrossRef](#)]
8. Dibenedetto, A.; Angelini, A.; Stufano, P. Use of carbon dioxide as feedstock for chemicals and fuels: Homogeneous and heterogeneous catalysis. *J. Chem. Technol. Biotechnol.* **2014**, *89*, 334–353. [[CrossRef](#)]
9. Holscher, M.; Gurtler, C.; Keim, W.; Muller, T.E.; Peters, M.; Leitner, W. Carbon dioxide as a carbon resource—Recent trends and perspectives. *Zeitschrift Für Naturforschung* **2012**, *67b*, 961–975. [[CrossRef](#)]
10. Ghanbari, T.; Abnisa, F.; Wan Daud, W.M.A. A review on production of metal organic frameworks (MOF) for CO₂ adsorption. *Sci. Total Environ.* **2020**, *707*, 135090:1–135090:28. [[CrossRef](#)]
11. Shi, Y.; Hou, S.; Qiu, X.; Zhao, B. MOFs-based catalysts supported chemical conversion of CO₂. *Top. Curr. Chem.* **2020**, *378*, 11:1–11:54. [[CrossRef](#)]
12. Thomas, I.R.; Bruno, I.J.; Cole, J.C.; Macrae, C.F.; Pidcock, E.; Wood, P.A. *WebCSD: The online portal to the Cambridge Structural Database.* *J. Appl. Cryst.* **2010**, *43*, 362–366. [[CrossRef](#)] [[PubMed](#)]
13. Shaikh, A.-A.G.; Sivaram, S. Organic carbonates. *Chem. Rev.* **1996**, *96*, 951–976. [[CrossRef](#)] [[PubMed](#)]
14. Fiorani, G.; Perosa, A.; Selva, M. Dimethyl carbonate: A versatile reagent for a sustainable valorization of renewables. *Green Chem.* **2018**, *20*, 288–322. [[CrossRef](#)]
15. Esan, A.O.; Adeyemi, A.D.; Ganesan, S. A review on the recent application of dimethyl carbonate in sustainable biodiesel production. *J. Clean. Prod.* **2020**, *257*, 120561:1–120561:21. [[CrossRef](#)]
16. Tamboli, A.H.; Chaugule, A.A.; Kim, H. Catalytic developments in the direct dimethyl carbonate synthesis from carbon dioxide and methanol. *Chem. Eng. J.* **2017**, *323*, 530–544. [[CrossRef](#)]
17. Kizlink, J. Synthesis of dimethyl carbonate from carbon dioxide and methanol in the presence of organotin compounds. *Collect. Czechoslov. Chem. Commun.* **1993**, *48*, 1399–1402. [[CrossRef](#)]
18. Kizlink, J.; Pastucha, I. Preparation of dimethyl carbonate from methanol and carbon dioxide in the presence of organotin compounds. *Collect. Czechoslov. Chem. Commun.* **1994**, *59*, 2116–2118. [[CrossRef](#)]
19. Kizlink, J.; Pastucha, I. Preparation of dimethyl carbonate from methanol and carbon dioxide in the presence of Sn(IV) and Ti(IV) alkoxides and metal acetates. *Collect. Czech. Chem. Commun.* **1995**, *60*, 687–692. [[CrossRef](#)]
20. Bloodworth, A.J.; Davies, A.G.; Vasishtha, S.C. Organometallic reactions. Part VII. Further addition reactions of Tributyltin Methoxide and of Bistributyltin oxide. *J. Chem. Soc. C* **1967**, 1309–1313. [[CrossRef](#)]
21. Blunden, S.J.; Hill, R.; Ruddick, J.N. The structure of bis(trialkyltin) carbonates: Evidence for two non-equivalent tin sites. *J. Organomet. Chem.* **1984**, *267*, C5–C8. [[CrossRef](#)]
22. Ballivet-Tkatchenko, D.; Douteau, O.; Stutzmann, S. Reactivity of carbon dioxide with *n*-Butyl(phenoxy)-, (alkoxy)-, and (oxo)stannanes: Insight into dimethyl carbonate synthesis. *Organometallics* **2000**, *19*, 4563–4567. [[CrossRef](#)]
23. Choi, J.-C.; Sakakura, T.; Sako, T. Reaction of dialkyltin methoxide with carbon dioxide relevant to the mechanism of catalytic carbonate synthesis. *J. Am. Chem. Soc.* **1999**, *121*, 3793–3794. [[CrossRef](#)]

24. Chambrey, S. Valorisation Chimique du Dioxyde de Carbone–Synthon et Solvant en Catalyse Moléculaire Pour la Synthèse de Carbonates de Dialkyle. Ph.D. Thesis, University of Burgundy, Dijon, France, 2007.
25. Ballivet-Tkatchenko, D.; Chermette, H.; Plasseraud, L.; Walter, O. Insertion reaction of carbon dioxide into Sn–OR bond. Synthesis, structure and DFT calculations of di- and tetranuclear isopropylcarbonato tin(IV) complexes. *Dalton Trans.* **2006**, *43*, 5167–5175. [[CrossRef](#)] [[PubMed](#)]
26. Plasseraud, L.; Catey, H.; Richard, P.; Ballivet-Tkatchenko, D. A novel two-dimensional organostannoxane coordination network promoted by phenazine: Synthesis, characterization and X-ray structure of $^2_{\infty}\{[n\text{-Bu}_2(\mu\text{-OH})\text{SnOSn}(\mu\text{-}\eta^2\text{-O}_3\text{SCF}_3)n\text{-Bu}_2]_2[n\text{-Bu}_2(\eta^1\text{-O}_3\text{SCF}_3)\text{SnOSn}(\mu\text{-OH})n\text{-Bu}_2]_2\}$. *J. Organomet. Chem.* **2009**, *694*, 2386–2394. [[CrossRef](#)]
27. Laurenczy, G.; Dalebrook, A.F.; Picquet, M.; Plasseraud, L. High-pressure NMR spectroscopy: An in situ tool to study tin-catalyzed synthesis of organic carbonates from carbon dioxide and alcohols. Part 2. *J. Organomet. Chem.* **2015**, *796*, 53–58. [[CrossRef](#)]
28. Ballivet-Tkatchenko, D.; Jerphagnon, T.; Ligabue, R.; Plasseraud, L.; Poinot, D. The role of distannoxanes in the synthesis of dimethyl carbonate from carbon dioxide. *Appl. Catal. Gen.* **2003**, *255*, 93–99. [[CrossRef](#)]
29. Wakamatsu, K.; Orita, A.; Otera, J. DFT Study on activation of carbon dioxide by dimethyltin dimethoxide for synthesis of dimethyl carbonate. *Organometallics* **2010**, *29*, 1290–1295. [[CrossRef](#)]
30. Poor Kalhor, M.; Chermette, H.; Chambrey, S.; Ballivet-Tkatchenko, D. From CO₂ to dimethyl carbonate with dialkyldimethoxystannanes: The key role of monomeric species. *Phys. Chem. Chem. Phys.* **2011**, *13*, 2401–2408. [[CrossRef](#)]
31. Poor Kalhor, M.; Chermette, H.; Ballivet-Tkatchenko, D. Reactivity of dialkoxydibutylstannanes toward carbon dioxide: A DFT study of electronic and steric effects. *Polyhedron* **2012**, *32*, 73–77. [[CrossRef](#)]
32. Ballivet-Tkatchenko, D.; Bernard, F.; Demoisson, F.; Plasseraud, L.; Sanapureddy, S.R. Tin-Based mesoporous silica for the conversion of CO₂ into dimethyl carbonate. *ChemSusChem* **2011**, *4*, 1316–1322. [[CrossRef](#)]
33. Kulmiz, P.J. Ueber Methstannäthyloxyd und dessen Verbindungen. *Prakt. Chem.* **1860**, *80*, 60–101. [[CrossRef](#)]
34. Lohmann, D.H. The infrared spectra of ethyltin compounds in the region 2–45 μ . *J. Organomet. Chem.* **1965**, *4*, 382–391. [[CrossRef](#)]
35. Sato, H. A Bridge-type Sn \cdots O Coordination of Bis(trialkyltin) Carbonates. *Bull. Chem. Soc. Jpn.* **1967**, *40*, 410–411. [[CrossRef](#)]
36. Lockhart, T.P. Steric effects in neophyltin(IV) chemistry. *J. Organomet. Chem.* **1985**, *287*, 179–186. [[CrossRef](#)]
37. Tiekink, E.R.T. The crystal structure of bis(trimethyltin)carbonate). *J. Organomet. Chem.* **1986**, *302*, C1–C3. [[CrossRef](#)]
38. Kümmerlen, J.; Sebal, A.; Reuter, H. The structure of (t-Bu₃Sn)₂CO₃ and (Me₃Sn)₂CO₃ in solution and in the solid state studied by ¹³C/¹¹⁹Sn NMR spectroscopy and X-ray diffraction. *J. Organomet. Chem.* **1992**, *427*, 309–323. [[CrossRef](#)]
39. Li, S.-L.; Ping, G.-J.; Liu, J.; Ma, J.-F.; Su, Z.-M. A novel chiral 3D supramolecular framework based on organooxotin cluster. *Inorg. Chem. Commun.* **2008**, *11*, 220–224. [[CrossRef](#)]
40. Ghionoiu, A.-E.; Popescu, D.-L.; Maxim, C.; Madalan, A.M.; Haiduc, I.; Andruh, M. Atmospheric CO₂ capture by a triphenyltin–1,2-bis(4-pyridyl)ethane system with formation of a rare trinuclear carbonato-centered core. *Inorg. Chem. Commun.* **2015**, *58*, 71–73. [[CrossRef](#)]
41. Goel, R.G.; Prasad, H.S.; Bancroft, G.M.; Sham, T.K. Preparation, Mössbauer and vibrational spectra of diorganotin chromates and carbonates. *Can. J. Chem.* **1976**, *54*, 711–717. [[CrossRef](#)]
42. Smith, P.J.; Hill, R.; Nicolaides, A.; Donaldson, J.D. Preparation and spectroscopic studies of diorganotin oxycarbonates. *J. Organomet. Chem.* **1983**, *252*, 149–152. [[CrossRef](#)]
43. Knoll, S.; Tschwatschalb, F.; Ristaub, T.; Gelbrichb, T.; Borsdorf, R. Diorganotin(IV) derivatives of tridentate dithiocarbazones—Structure determination in the solid and liquid state. *Z. Anorg. Allg. Chem.* **1997**, *623*, 141–146. [[CrossRef](#)]
44. Holmes, R.R. Organotin cluster chemistry. *Acc. Chem. Res.* **1989**, *22*, 190–197. [[CrossRef](#)]
45. Chandrasekhar, V.; Nagendran, S.; Baskar, V. Organotin assemblies containing Sn–O bonds. *Coord. Chem. Rev.* **2002**, *235*, 1–52. [[CrossRef](#)]
46. Zheng, G.-L.; Ma, J.-F.; Yang, J.; Li, Y.-Y.; Hao, X.-R. New system in organooxotin cluster chemistry incorporating inorganic and organic spacers between two ladders each containing five tin atoms. *Chem. Eur. J.* **2004**, *10*, 3761–3768. [[CrossRef](#)] [[PubMed](#)]

47. Plasseraud, L.; Cattey, H.; Richard, P. Unprecedented Hexa- and undecanuclear frameworks of two new Tin(IV) oxo clusters resulting from partial Debenzylation reactions. *Z. Naturforsch. B* **2010**, *65*, 1293–1300. [[CrossRef](#)]
48. Ballivet-Tkatchenko, D.; Chambrey, S.; Keiski, R.; Ligabue, R.; Plasseraud, L.; Richard, P.; Turunen, H. Direct synthesis of dimethyl carbonate with supercritical carbon dioxide: Characterization of a key organotin oxide intermediate. *Catal. Today* **2006**, *115*, 80–87. [[CrossRef](#)]
49. Sanapureddy, S.R.; Plasseraud, L. (*n*-Bu₂Sn)₂O(CO₃): An active, robust and recyclable organotin(IV) for the direct synthesis of linear organic carbonates from carbon dioxide and alcohols. *Appl. Organomet. Chem.* **2017**, *31*, e3807:1–e3807:8. [[CrossRef](#)]
50. Plasseraud, L.; Ballivet-Tkatchenko, D.; Cattey, H.; Chambrey, S.; Ligabue, R.; Richard, P.; Willem, R.; Biesemans, M. Di-*n*-butyltin oxide as a chemical carbon dioxide capturer. *J. Organomet. Chem.* **2010**, *695*, 1618–1626. [[CrossRef](#)]
51. Reuter, H.; Wilberts, H. On the structural diversity anions coordinate to the butterfly-shaped [(R₂Sn)₃O(OH)₂]²⁺ cations and vice versa. *Can. J. Chem.* **2014**, *92*, 496–507. [[CrossRef](#)]
52. Ballivet-Tkatchenko, D.; Burgat, R.; Chambrey, S.; Plasseraud, L.; Richard, P. Reactivity of ditert-butyl dimethoxystannane with carbon dioxide and methanol: X-ray structure of the resulting complex. *J. Organomet. Chem.* **2006**, *691*, 1498–1504. [[CrossRef](#)]
53. Ahmad, S.U.; Beckmann, J.; Duthie, A. New insights into the formation and reactivity of molecular organostannonic acids. *Chem. Asian J.* **2010**, *5*, 160–168. [[CrossRef](#)] [[PubMed](#)]
54. Švec, P.; Cattey, H.; Růžičková, Z.; Holub, J.; Růžička, A.; Plasseraud, L. Triorganotin(IV) cation-promoted dimethyl carbonate synthesis from CO₂ and methanol: solution and solid-state characterization of an unexpected diorganotin(IV)-oxo cluster. *New J. Chem.* **2018**, *42*, 8253–8260. [[CrossRef](#)]
55. Beckmann, J.; Dakternieks, D.; Duthie, A.; Lewcenko, N.A.; Mitchell, C. Carbon dioxide fixation by the cooperative effect of organotin and organotellurium oxides. *Angew. Chem. Int. Ed.* **2004**, *43*, 6683–6685. [[CrossRef](#)] [[PubMed](#)]
56. Beckmann, J.; Dakternieks, D.; Duthie, A.; Mitchell, C. A dimeric tellurastannoxane carbonate cluster, tetra-*tert*-butyl-di- μ_3 -carbonato-tetrakis-[4-(*N,N*-dimethylamino)phenyl]di- μ -oxo-ditelluriumditin chloroform tetrasolvate. *Acta Cryst.* **2004**, *E60*, m1978–m1979.
57. Ahmad, S.U.; Beckmann, J.; Duthie, A. Hexameric methylstannoxyl carbonate ion [MeSn(O)CO₃]₆⁶⁻ a missing link with a drum-type structure. *Organometallics* **2009**, *28*, 7053–7054. [[CrossRef](#)]
58. Yoshida, M.; Ueki, T.; Yasuoka, N.; Kasai, N.; Kakudo, M.; Omae, I.; Kikkawa, S.; Matsuda, S. The crystal and molecular structure of an isomer of Bis-(1,2-diethoxycarbonyl-ethyl)tin dibromide. *Bull. Chem. Soc. Jpn.* **1968**, *41*, 1113–1119. [[CrossRef](#)]
59. Jastrzebski, J.T.B.H.; van Koten, G. Intramolecular coordination in organotin Chemistry. *Adv. Organomet. Chem.* **1993**, *35*, 241–294.
60. Padělková, Z.; Weidlich, T.; Kolářová, L.; Eisner, A.; Císařová, I.; Zevaco, T.A.; Růžička, A. Products of hydrolysis of C,*N*-chelated triorganotin(IV) chlorides and use of products as catalysts in transesterification reactions. *J. Organomet. Chem.* **2007**, *692*, 5633–5645. [[CrossRef](#)]
61. Švec, P.; Olejník, R.; Padělková, Z.; Růžička, A.; Plasseraud, L.; Olejník, R.; Padělková, Z.; Růžička, A.; Plasseraud, L. C,*N*-chelated organotin(IV) trifluoromethanesulfonates: Synthesis, characterization and preliminary studies of its catalytic activity in the direct synthesis of dimethyl carbonate from methanol and CO₂. *J. Organomet. Chem.* **2012**, *7087–09*, 82–87.
62. Padělková, Z.; Vaňkátová, H.; Císařová, I.; Nechaev, M.S.; Zevaco, T.A.; Walter, O.; Růžička, A. Reactivity of a C,*N*-chelated stannoxane. *Organometallics* **2009**, *28*, 2629–2632. [[CrossRef](#)]
63. Mairyčová, B.; Dostál, L.; Růžička, A.; Beneš, L.; Jambor, R. Reversible CO₂ fixation by intramolecularly coordinated diorganotin(IV) oxides. *J. Organomet. Chem.* **2012**, *699*, 1–4. [[CrossRef](#)]
64. Simón-Manso, E.; Kubiak, C.P. A trihydroxy tin group that resists oligomerization in the trinuclear nickel cluster [Ni₃(μ -P-P'-PPh₂CH₂PPh₂)₃(μ_3 -L)-(μ_3 -Sn(OH)₃)]. *Angew. Chem.* **2005**, *117*, 1149–1152. [[CrossRef](#)]

